Histological analyses of the muscle injected with the three-morpholino cocktail (1.2mg/each) showed significant histological improvement of the dystrophy, relative to uninjected muscle, (see Fig 3A; bottom panels).

By immunoblotting, intramuscular injection of the optimal cocktail induced dystrophin to 50% normal levels in a 2-year-old dog but only to 25% in a more clinically severe 5-year-old dog (see Supplemental Fig 2A). This result implies that the muscle quality influences the amount of dystrophin that can be produced.

Intravenous Systemic Delivery of a Morpholino Cocktail Induces Body-Wide Dystrophin Expression

AOs must be deliverable systemically to be of therapeutic value. Accordingly, we undertook intravenous infusion of the three morpholino-cocktail showing the most success in the intramuscular experiments (Ex6A, Ex6B, and Ex8A). Three CXMD dogs were studied using intravenous doses similar to that used in *mdx* mouse studies (30–40mg/kg per injection), with weekly or biweekly dosing. The first dog received 120mg/kg morpholinos (40mg/kg per each sequence) in weekly intravenous injections, with five doses over 5 weeks. The second dog was given the same dose 11 times at 2-week intervals over the course of 5.5 months. The third dog received a greater dose: 200mg/kg (66mg/kg of each morpholino) seven times at weekly intervals (see the Supplementary Table). All dogs were euthanized 2 weeks after the last injection, and multiple muscles were examined.

All skeletal muscles of each treated dog showed evidence of *de novo* dystrophin expression by immunofluorescence of cryosections, although the degree of rescue was variable (Fig 4A). Histopathology was markedly improved in regions showing high dystrophin expression (see Fig 4A). Immunoblotting confirmed expression up to approximately 50% of normal levels, but some muscles expressed only trace amounts (see Figs 4C, D). Dystrophin expression was also detected in cardiac muscles but, as in the *mdx* mouse,[19] less than in skeletal muscles and concentrated in small patches (see Fig 4A). Of the three dogs, the average dystrophin protein expression level was greatest in the dog given seven weekly doses of 200mg/kg PMO, with an average of 26% of normal dystrophin levels.

Selected muscles were studied for quantitative rescue of histopathology and for biochemical rescue of dystrophin-interacting proteins (dystrophin-associated glycoproteins and nNOS). A commonly utilized quantitative marker for muscle pathology is central nucleation of myofibers, where increased central nucleation is reflective of increased degeneration and regeneration. Quantitation of central nucleation in treated dogs compared with untreated littermates showed that intravenous antisense treatment reduced central nucleation in all five muscle groups examined (see Fig 4B).

Both nNOS and α-sarcoglycan are dystrophin-associated proteins that colocalize with dystrophin in normal muscle and are reduced in DMD muscle. nNOS immunofluorescence and α-sarcoglycan immunoblotting were done on a series of muscles from treated and control dogs. By immunoblot, α-sarcoglycan was seen to be increased in all muscles examined (Fig 5B). Likewise, nNOS was seen to relocalize to the membrane in dystrophin-positive regions in systemically treated dogs (see Fig 5A).

Muscle Imaging and Clinical Grading Scores Are Improved by Systemic Antisense Treatment

A global improvement in muscle pathology was further supported by the T2-weighted MRI examination (Fig 6). The high-intensity T2 signal, indicative of inflammation and increased water content, was diminished in PMO-treated dogs compared with pretreated and untreated control dogs in most muscles (see Fig 6).

Functional improvement of treated dogs was also assessed by a 15m timed running test and by a combined clinical grading score, as we have previously published.[18] Three dogs treated with intravenous morpholinos were compared with three untreated, at the ages of both 2 or 5 months (pretreatment) and 4 or 7 months (posttreatment) (Figs 7B, C). The untreated littermates became slower over the treatment time, whereas all treated dogs ran faster after treatment. The single dog treated at an older age with more advanced symptoms showed greater improvement relative to untreated littermates (see Fig 7B).

The combined clinical grading score similarly showed improvement or stabilization of disease progression after antisense treatment, relative to natural history controls (see Fig 7A). Videos documenting running ability of treated dogs and untreated littermates are available as supplemental data (see Supplemental Movies 1–5).

Serum creatine kinase was assessed before and after intravenous treatment, and compared with natural history controls (see Supplemental Fig 3). Although serum creatine kinase was variable, posttreatment creatine kinase levels were consistently less than natural history controls.

Intravenous High-Dose Morpholino Cocktail Shows No Evidence of Toxicity

No local inflammatory reactions or organ dysfunctions were recorded in the morpholino-treated dogs. Twice-weekly serum toxicology screens of the three systemically treated dogs showed no evidence of liver or kidney dysfunction (see Supplemental Fig 4). Levels of urea nitrogen, α-glutamyl transpeptidase, and creatinine all remained within the reference ranges. In addition, no significant changes were observed in amylase, total protein, total bilirubin, C-reactive protein, sodium, potas-

sium, or chloride. Growth of body weight was also within reference range in all treated dogs (data not shown).

Discussion

This is the first report of widespread induction of dystrophin expression to therapeutic levels in the dog model of DMD. Overall, our findings provide a promising message for DMD patients. Specifically, we show that intravenous morpholino antisense (PMOs) can generate body-wide production of functional dystrophin in a model clinically more severe than DMD, resulting in stabilization or improvement of the clinical disease. Beneficial effects were documented by histology, MRI, and functional tests (running and combined clinical grading scores).

We encountered some unexpected findings that raise important questions as to how to pursue this promising approach into human clinical trials. Clearly, the choice of specific antisense sequences is a crucial determinant of the ultimate success of targeted exon skipping. To date, specific AO sequences have been assessed for efficiency of exon skipping using cell-based experimental (*in vitro*) systems, with the optimal sequences then used for *in vivo* experiments. In studies presented here, antisense oligonucleotides directed against exon 6 were able to efficiently induce the desired exon 5 to 10 splicing *in vitro* but not *in vivo*. Our observations of discrepant outcomes for *ex vivo* and *in vivo* in the dystrophic dog tell us that we do not currently possess a reliable means of screening for sequences that induce efficient skipping of a particular exon in a particular mutational context. Data obtained from application of sequences as 2'O-MePs in primary myogenic cells or as PMOs incubated *ex vivo* with muscle fragments failed to predict the effects when PMO sequences were tested *in vivo*. The high percentage of in-frame products here might be related to nonsense-mediated decay of out-of-frame products or quality of RNA from cell culture; however, the *in vitro* experiments were consistent using three different concentrations (600, 60, and 30nM) with two different sequences (Ex6A and Ex6B). The results were confirmed by RT-PCR, immunohistochemistry, and complementary DNA sequences (see Fig 2; see Supplemental Fig 1). The *in vitro* effect of

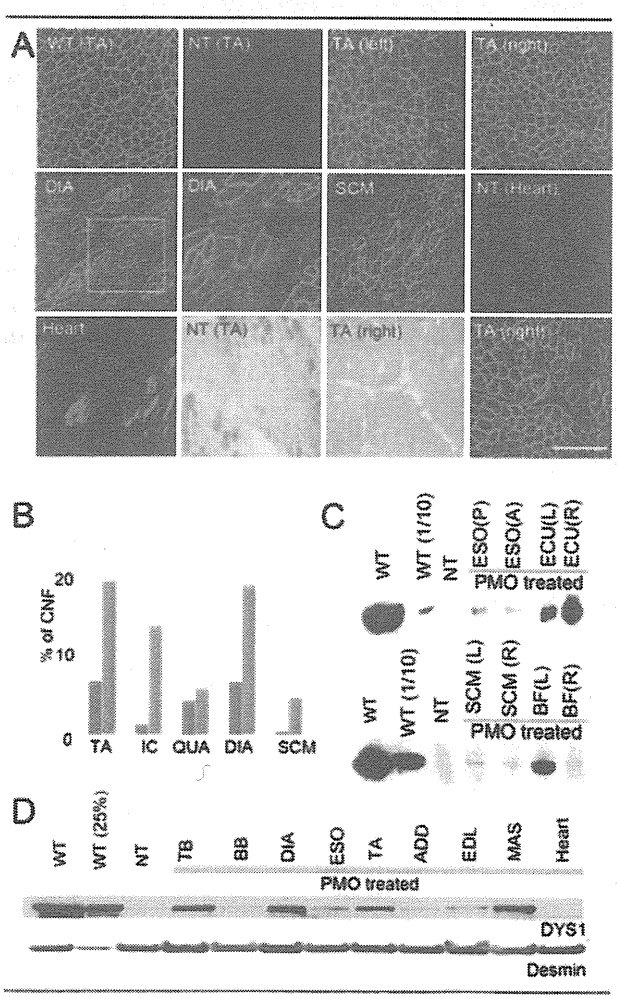

Fig 4. Widespread dystrophin expression and improved histology by intravenous systemic delivery of cocktail morpholinos in canine X-linked muscular dystrophy (CXMD) dogs. (A) Dystrophin (DYS-1) staining and histology in bilateral tibialis anterior muscles (TA), diaphragm (DIA), sternocleidomastoid (SCM), and heart at 2 weeks after final injection after five weekly intravenous injections of 120mg/kg cocktail morpholinos containing Ex6A, Ex6B, and Ex8A (2001MA). Comparisons were made with TA from normal control animal (wild type [WT]) and from nontreated CXMD littermate (NT) tibialis anterior (TA) and heart. Intravenous morpholino treatment resulted in extensive, though variable, dystrophin production in multiple muscles, but with only limited evidence of rescue in heart (isolated cardiocytes). Paired dystrophin immunostaining and histology from treated dog (TA, bottom panels) showed improved histopathology relative to untreated littermate (NT TA) histology. Bars = 200μm, except for higher magnification picture of DIA and hearts (100μm). (B) Quantitation of centrally nucleated fibers (CNFs) in TA, intercostal (IC), quadriceps (QUA), diaphragm (DIA), and sternocleidomastoid (SCM) in treated dog (blue bars; *2001MA) and untreated dog (red bars; 2008MA). (C) Western blotting analysis for detection of dystrophin at 2 weeks after final injection after 5 × weekly intravenous injections of 120mg/kg cocktail morpholinos containing Ex6A, Ex6B, and Ex8A (2001MA). Dystrophin rescue is variable with high expression in right extensor carpi ulnaris [ECU(R)] and left biceps femoris [BF(L)], and less in posterior [ESO(P)] or anterior esophagus [ESO(A)] and sternocleidomastoid (SCM). (D) Immunoblot analysis of dystrophin in intravenous morpholino-treated dog (2703MA; 7 × weekly dosing) and control animals (normal control [WT], nontreated [NT]). Desmin immunoblot is shown as a loading control. Dystrophin shows high levels (>25% control levels) in triceps brachii (TB), DIA, and masseter (MAS). ADD = adductor; BB = biceps brachii; EDL = extensor digitorum longus; MAS = masseter.*

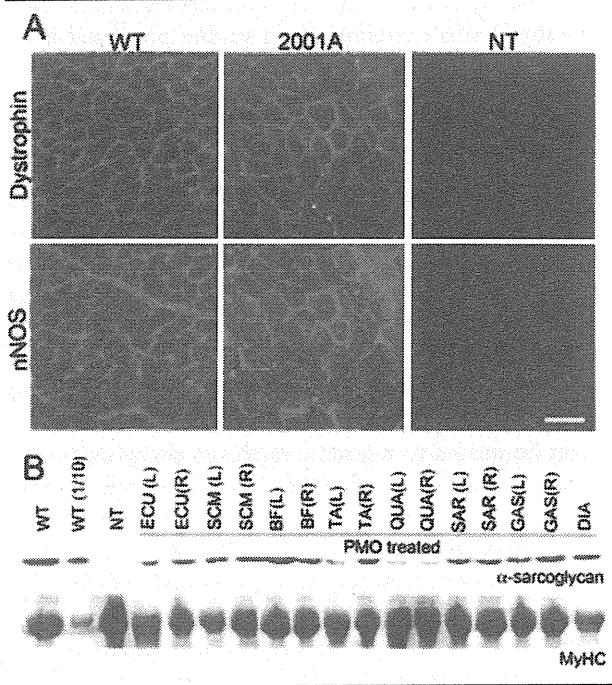

Fig 5. Recovery of localization and expression of dystrophin-associated proteins after systemic delivery of cocktail morpholinos to canine X-linked muscular dystrophy (CXMD) dogs. Neuronal nitric oxide synthase (nNOS) (A) and α-sarcoglycan (B) expression at 2 weeks after 5 × weekly 120mg/kg cocktail (2001MA) or 7 × weekly 200mg/kg cocktail morpholino injections (2703MA) to CXMD dogs. Recovery of nNOS expression at sarcolemma was observed by double immunofluorescence against dystrophin (DYS-1) and nNOS. Scale bar = 50μm. By immunoblot (B), α-sarcoglycan levels are increased in treated dog muscles, compared with untreated dystrophic controls (NT). Myosin heavy chain (MyHC) shown as a loading control. WT = wild-type normal control animals; WT(1/10) = wild-type (1/10 diluted samples, ie, 4μg loaded); NT = nontreated CXMD muscles (tibialis anterior); ECU = extensor carpi ulnaris; SCM = sternocleidomastoid; BF = biceps femoris; TA = tibialis anterior; QUA = quadriceps; SAR = sartorius; GAS = gastrocnemius; DIA = diaphragm; L = left side; R = right side.

the exon 6–specific sequence was, in addition, context dependent. For when transfected into wild-type Beagle myoblasts, the exon 8 AO pair again excised exons 8 and 9, whereas the exon 6–specific AO pair excised exons 6 and 9, leaving exons 7 and 8 in place (see Supplemental Fig 1). Thus, excision of exon 8 by the exon 6–specific sequences occurs only in the context of the mutant exon 7 splice site. Together, the differences between patterns of skipping *in vivo* versus *in vitro* and between wild-type versus mutant genotypes tell us that efficiency of skipping during transcription is dominated by variables other than the availability or otherwise of specific local sequence. Thus, it is prudent to consider testing of selected sequences in multiple systems with human dystrophin mRNA as the target before committing to a specific sequence for clinic trials.

We observed efficient skipping of exon 9, even though no antisense sequence targeted its removal in both wild-type and CXMD (see Figs 2 and 3), which is known as alternative splice site.[20] AOs targeting exon 8 have been reported to induce skipping of both exon 8 and 9 in human and in dog studies (see Figs 2 and 3).[10,21] It appears likely that the small size of intron 8 compared with intron 7 (1.1 vs 110Kb) predisposes to splicing of exon 8 to exon 9 before splicing to exon 7.

In the systemically treated dogs, we found widespread expression of dystrophin in all muscles analyzed but with considerable variation (see Fig 4). No difference in dystrophin expression between fiber types was evident

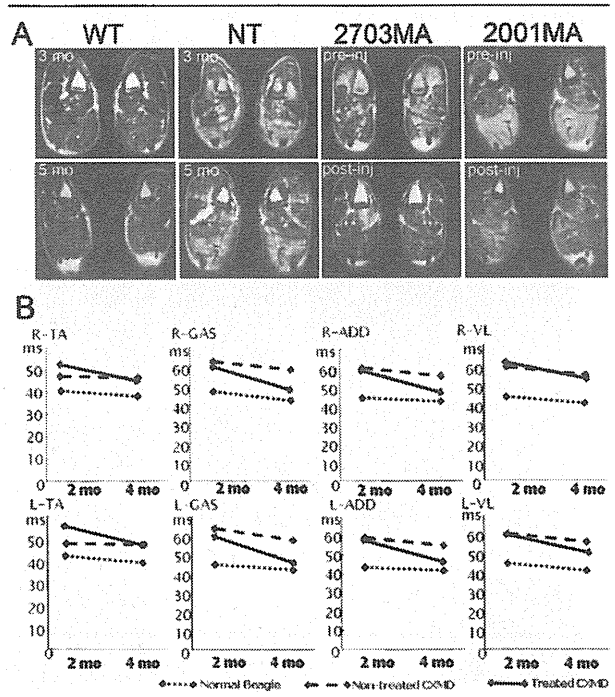

Fig 6. Amelioration of pathology and reduced inflammation signal in magnetic resonance imaging (MRI). T2-weighted MRI of hind legs at 1 week before initial injection (pre-inj) and at 2 weeks after final injection (post-inj) of 7 × weekly intravenous (IV) injection of 200mg/kg cocktail morpholinos (2703MA) or 5 × weekly IV injection of 120mg/kg cocktail morpholinos (2001MA). Age-matched untreated dogs (wild type [WT; normal control] and nontreated dystrophic control [NT]) are shown for comparison. (B) Changes of T2 value examined by MRI at 2 weeks after 7 × weekly 200mg/kg cocktail morpholino injections. Changes of T2 values in hind legs at 1 week before initial injection and at 2 weeks after final injection are shown. Intravenous morpholino treatment resulted in decreased T2 signal in all muscles examined. TA = tibialis anterior; GAS = gastrocnemius; ADD = adductor; VL = vastus lateralis. Dotted lines *represent normal Beagle;* dashed lines *represent nontreated canine X-linked muscular dystrophy (CXMD);* solid lines *represent treated CXMD.*

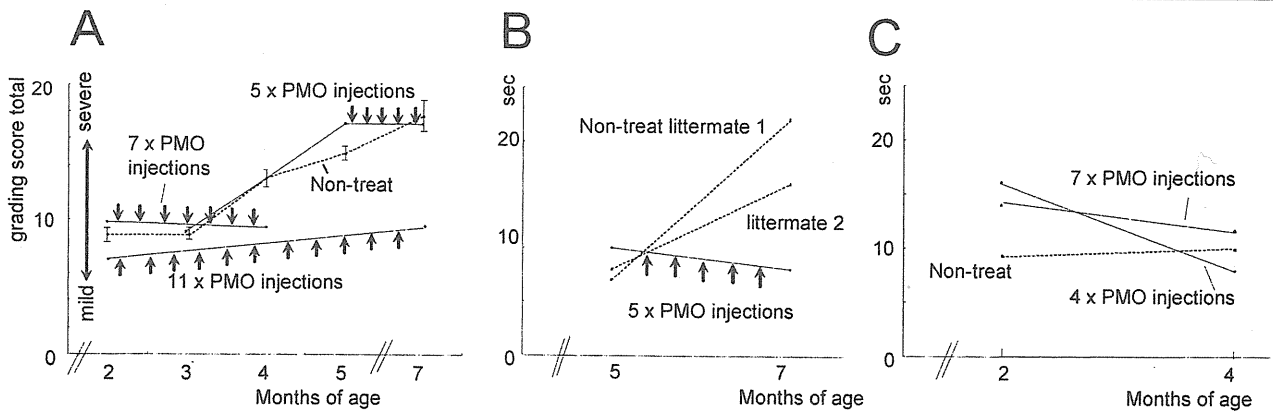

Fig 7. Stabilization of clinical symptoms by systemic morpholino treatment. (A) Combined clinical grading scores before (black lines) *and after starting treatment* (red lines) *of the three treated dogs. Clinical grades of gait disturbance, mobility disturbance, limb or temporal muscle atrophy, drooling, macroglossia, and dysphagia are scored as described in Materials and Methods. A series of untreated dogs (n = 6–13) was studied for comparison* (dashed line, *standard error bars). (B, C) Fifteen-meter timed running tests in treated dogs and untreated littermates. A canine X-linked muscular dystrophy (CXMD) dog treated from 5 to 7 months (2001MA) of age showed decreased timed 15m run after treatment, whereas untreated littermates showed slowed running ability (B). Similarly, two littermate dogs treated at 2 to 4 months of age (2703MA; 2702FA) showed quicker 15m times after treatment compared with nontreated littermate (C).*

(data not shown). Even contralateral muscles differed from one another, suggesting that variation in efficacy of dystrophin production is a reflection of transient sporadic events such as myopathic episodes or changes in vascularization or circulation rather than any intrinsic muscle-specific properties. Pathological stages of degeneration/regeneration may also be involved. Overall, most studies to date suggest that 10 to 20% normal dystrophin levels are needed to improve muscle function,[22,23] and the data on systemic morpholino-induced exon skipping presented here imply that some, but not all, muscle groups reached this therapeutic level.

Systemic delivery of morpholinos in CXMD dogs as in *mdx* mice induced only modest dystrophin production in the heart (see Fig 4).[19] The reason is not clear, but it has been suggested that dystrophic skeletal muscle fibers may give greater access to AOs because they have more "leaky" membranes than the smaller cardiac cells and because the syncytial structure of myofibers may permit wider diffusion of PMO molecules from each site of entry.[24] Cardiac ischemia, as indicated by abnormal Q-waves in CXMD,[25] may also limit access of AOs to cardiomyocytes. Some improvement in delivery has been reported with cell-penetrating peptide-tagged morpholinos, or use of microbubbles and ultrasound that may enhance uptake efficiency in the heart by facilitating penetration of cell membranes, although toxicity of these strategies is not clear.[26,27]

Considerable evidence for functional and histological improvement was seen in the three systemically treated dogs (see Figs 4–7). All were stabilized compared with their untreated littermates in motor function tests, general clinical condition, and serum creatine kinase levels. MRI images also showed reduction of T2-weighted signal, interpreted as a sign of diminished inflammation, after morpholino delivery (see Fig 6). However, longer-term experiments are required to investigate whether AOs can reduce infiltration by fibrofatty tissue and to what extent functional loss can be recovered.

Many DMD patients require two or more exons to be skipped to restore the reading frame. The data reported here are the first demonstrations of efficient skipping of multiple exons systemically through intravenous delivery. The dog model required skipping of two to three exons to restore the reading frame, and we were able to show efficient skipping of three exons by both intramuscular and intravenous delivery methods. Multiexon skipping has also been shown in *in vitro* cell cultures and in *mdx* mice by intramuscular injections.[8,28–30] Multiexon skipping increases the range of potentially treatable DMD patients and also raises the prospect of selecting the most functionally favorable in-frame dystrophins,[7] although skipping larger stretches of exons has yet not been achieved and currently may not be feasible. Specific morpholino cocktails able to treat a large proportion of DMD patients with optimized quasi-dystrophin production might be submitted for regulatory approval as a single "drug." For example, a cocktail of AOs targeting exons 45 to 55 would be applicable in up to 63% of patients with dystrophin deletions, and this specific deletion is associated with asymptomatic or mild BMD clinical phenotypes.[31,32]

This work was supported by the Foundation to Eradicate Duchenne, the Department of Defense CDMRP program (W81XWH-05-1-

0616 E.P.H.), the Jain Foundation (E.P.H.), the Crystal Ball of Virginia Beach (Muscular Dystrophy Association USA) (E.P.H.), the National Center for Medical Rehabilitation Research 5R24HD050846-02 (E.P.H.), the NIH Wellstone Muscular Dystrophy Research Centers IU54HD053177-01A1 (E.P.H.), and the Ministry of Health, Labor, and Welfare of Japan (Research on Nervous and Mental Disorders, 16B-2, 19A-7; Health and Labor Sciences, Research Grants for Translation Research, H19-translational research-003, Health Sciences Research Grants for Research on Psychiatry and Neurological Disease and Mental Health, H18-kokoro-019) (S.T.).

We thank Drs S. Duguez, J. Nazarian, H. Gordish-Dressman, Y. Aoki, T. Saito, K. Yuasa, N. Yugeta, S. Ohshima, Z.-H. Shin, MR. Wada, K. Fukushima, S. Masuda, K. Kinoshita, H. Kita, S. Ichikawa, Y. Yahata, T. Nakayama, A. Rabinowitz, and JR. Beauchamp for discussions and technical assistance.

References

1. Hoffman EP, Brown RH Jr, Kunkel LM. Dystrophin: the protein product of the Duchenne muscular dystrophy locus. Cell 1987;51:919–928.
2. Matsumura K, Campbell KP. Dystrophin-glycoprotein complex: its role in the molecular pathogenesis of muscular dystrophies. Muscle Nerve 1994;17:2–15.
3. Koenig M, Beggs AH, Moyer M, et al. The molecular basis for Duchenne versus Becker muscular dystrophy: correlation of severity with type of deletion. Am J Hum Genet 1989;45:498–506.
4. England SB, Nicholson LV, Johnson MA, et al. Very mild muscular dystrophy associated with the deletion of 46% of dystrophin. Nature 1990;343:180–182.
5. Dunckley MG, Manoharan M, Villiet P, et al. Modification of splicing in the dystrophin gene in cultured Mdx muscle cells by antisense oligoribonucleotides. Hum Mol Genet 1998;7:1083–1090.
6. van Deutekom JC, Janson AA, Ginjaar IB, et al. Local dystrophin restoration with antisense oligonucleotide PRO051. N Engl J Med 2007;357:2677–2686.
7. Yokota T, Duddy W, Partridge T. Optimizing exon skipping therapies for DMD. Acta Myol 2007;26:179–184.
8. Aartsma-Rus A, Janson AA, Kaman WE, et al. Antisense-induced multiexon skipping for Duchenne muscular dystrophy makes more sense. Am J Hum Genet 2004;74:83–92.
9. Sharp NJ, Kornegay JN, Van Camp SD, et al. An error in dystrophin mRNA processing in golden retriever muscular dystrophy, an animal homologue of Duchenne muscular dystrophy. Genomics 1992;13:115–121.
10. McClorey G, Moulton HM, Iversen PL, et al. Antisense oligonucleotide-induced exon skipping restores dystrophin expression in vitro in a canine model of DMD. Gene Ther 2006;13:1373–1381.
11. Shimatsu Y, Katagiri K, Furuta T, et al. Canine X-linked muscular dystrophy in Japan (CXMDJ). Exp Anim 2003;52:93–97.
12. Summerton J, Weller D. Morpholino antisense oligomers: design, preparation, and properties. Antisense Nucleic Acid Drug Dev 1997;7:187–195.
13. Yokota T, Takeda S, Lu QL, et al. A renaissance for anti-sense oligonucleotide drugs in neurology: exon-skipping breaks new ground. Arch Neurol 2009;66:32–38.
14. Jankowski RJ, Haluszczak C, Trucco M, Huard J. Flow cytometric characterization of myogenic cell populations obtained via the preplate technique: potential for rapid isolation of muscle-derived stem cells. Hum Gene Ther 2001;12:619–628.
15. Yokota T, Lu QL, Morgan JE, et al. Expansion of revertant fibers in dystrophic mdx muscles reflects activity of muscle precursor cells and serves as an index of muscle regeneration. J Cell Sci 2006;119:2679–2687.
16. Abramoff MD, Magelhaes PJ, Ram SJ. Image processing with ImageJ. Biophotonics Int 2004;11:36–42.
17. Araishi K, Sasaoka T, Imamura M, et al. Loss of the sarcoglycan complex and sarcospan leads to muscular dystrophy in beta-sarcoglycan-deficient mice. Hum Mol Genet 1999;8:1589–1598.
18. Shimatsu Y, Yoshimura M, Yuasa K, et al. Major clinical and histopathological characteristics of canine X-linked muscular dystrophy in Japan, CXMDJ. Acta Myol 2005;24:145–154.
19. Alter J, Lou F, Rabinowitz A, et al. Systemic delivery of morpholino oligonucleotide restores dystrophin expression bodywide and improves dystrophic pathology. Nat Med 2006;12:175–177.
20. Reiss J, Rininsland F. An explanation for the constitutive exon 9 cassette splicing of the DMD gene. Hum Mol Genet 1994;3:295–298.
21. Aartsma-Rus A, De Winter CL, Janson AA, et al. Functional analysis of 114 exon-internal AONs for targeted DMD exon skipping: indication for steric hindrance of SR protein binding sites. Oligonucleotides 2005;15:284–297.
22. Yoshimura M, Sakamoto M, Ikemoto M, et al. AAV vector-mediated microdystrophin expression in a relatively small percentage of mdx myofibers improved the mdx phenotype. Mol Ther 2004;10:821–828.
23. Liang KW, Nishikawa M, Liu F, et al. Restoration of dystrophin expression in mdx mice by intravascular injection of naked DNA containing full-length dystrophin cDNA. Gene Ther 2004;11:901–908.
24. Yokota T, Pistilli E, Duddy W, Nagaraju K. Potential of oligonucleotide-mediated exon-skipping therapy for Duchenne muscular dystrophy. Exp Opin Biol Ther 2007;7:831–842.
25. Yugeta N UN, Fujii Y, Yoshimura M, et al. Cardiac involvement in Beagle-based canine X-linked muscular dystrophy in Japan (CXMDJ): electrocardiographic, echocardiographic, and morphologic studies. BMC Cardiovasc Disord 2006;6:47.
26. Jearawiriyapaisarn N, Moulton HM, Buckley B, et al. Sustained dystrophin expression induced by peptide-conjugated morpholino oligomers in the muscles of mdx mice. Mol Ther 2008;16:1624–1629.
27. Vannan M, McCreery T, Li P, et al. Ultrasound-mediated transfection of canine myocardium by intravenous administration of cationic microbubble-linked plasmid DNA. J Am Soc Echocardiogr 2002;15:214–218.
28. Fall AM, Johnsen R, Honeyman K, et al. Induction of revertant fibres in the mdx mouse using antisense oligonucleotides. Genet Vaccines Ther 2006;4:3.
29. Aartsma-Rus A, Janson AA, van Ommen GJ, van Deutekom JC. Antisense-induced exon skipping for duplications in Duchenne muscular dystrophy. BMC Med Genet 2007;8:43.
30. Aartsma-Rus A, Kaman WE, Weij R, et al. Exploring the frontiers of therapeutic exon skipping for Duchenne muscular dystrophy by double targeting within one or multiple exons. Mol Ther 2006;14:401–407.
31. Nakamura A, Yoshida K, Fukushima K, et al. Follow-up of three patients with a large in-frame deletion of exons 45-55 in the Duchenne muscular dystrophy (DMD) gene. J Clin Neurosci 2008;15:757–763.
32. Beroud C, Tuffery-Giraud S, Matsuo M, et al. Multiexon skipping leading to an artificial DMD protein lacking amino acids from exons 45 through 55 could rescue up to 63% of patients with Duchenne muscular dystrophy. Hum Mutat 2007;28:196–202.

MECHANISMS OF DEVELOPMENT 126 (2009) 107–116

available at www.sciencedirect.com

ScienceDirect

journal homepage: www.elsevier.com/locate/modo

Reduced proliferative activity of primary POMGnT1-null myoblasts *in vitro*

Yuko Miyagoe-Suzuki[a,*], *Nami Masubuchi*[a,b], *Kaori Miyamoto*[a,b], *Michiko R. Wada*[a], *Shigeki Yuasa*[c], *Fumiaki Saito*[d], *Kiichiro Matsumura*[d], *Hironori Kanesaki*[e], *Akira Kudo*[e], *Hiroshi Manya*[f], *Tamao Endo*[f], *Shin'ichi Takeda*[a]

[a]*Department of Molecular Therapy, National Institute of Neuroscience, National Center of Neurology and Psychiatry, 4-1-1 Ogawahigashi, Kodaira, Tokyo 187-8502, Japan*
[b]*Molecular Embryology, Department of Biosciences, School of Science, Kitasato University, Kanagawa 228-8555, Japan*
[c]*Department of Ultrastructural Research, National Institute of Neuroscience, National Center of Neurology and Psychiatry, 4-1-1 Ogawahigashi, Kodaira, Tokyo 187-8502, Japan*
[d]*Department of Neurology and Neuroscience, Teikyo University School of Medicine, 2-11-1 Kaga, Itabashi-ku, Tokyo 173-8605, Japan*
[e]*Department of Biological Information, Tokyo Institute of Technology, Yokohama 226-8501, Japan*
[f]*Glycobiology Research Group, Tokyo Metropolitan Institute of Gerontology, Foundation for Research on Aging and Promotion of Human Welfare, 35-2 Sakaecho, Itabashi-ku, Tokyo 173-0015, Japan*

ARTICLE INFO

Article history:
Received 28 May 2008
Received in revised form
6 November 2008
Accepted 2 December 2008
Available online 16 December 2008

Keywords:
POMGnT1
Muscle–eye–brain disease
Satellite cells
Skeletal muscle
α-Dystroglycan
Glycosylation
Laminin

ABSTRACT

Protein O-linked mannose β1,2-*N*-acetylglucosaminyltransferase 1 (POMGnT1) is an enzyme that transfers *N*-acetylglucosamine to *O*-mannose of glycoproteins. Mutations of the *POMGnT1* gene cause muscle–eye–brain (MEB) disease. To obtain a better understanding of the pathogenesis of MEB disease, we mutated the *POMGnT1* gene in mice using a targeting technique. The mutant muscle showed aberrant glycosylation of α-DG, and α-DG from mutant muscle failed to bind laminin in a binding assay. *POMGnT1*$^{-/-}$ muscle showed minimal pathological changes with very low-serum creatine kinase levels, and had normally formed muscle basal lamina, but showed reduced muscle mass, reduced numbers of muscle fibers, and impaired muscle regeneration. Importantly, *POMGnT1*$^{-/-}$ satellite cells proliferated slowly, but efficiently differentiated into multinuclear myotubes *in vitro*. Transfer of a retrovirus vector-mediated *POMGnT1* gene into *POMGnT1*$^{-/-}$ myoblasts completely restored the glycosylation of α-DG, but proliferation of the cells was not improved. Our results suggest that proper glycosylation of α-DG is important for maintenance of the proliferative activity of satellite cells *in vivo*.

1. Introduction

POMGnT1 is the glycosyltransferase that catalyzes the transfer of *N*-acetylglucosamine (GlcNAc) to *O*-mannose of glycoproteins, the second step of Ser/Thr *O*-mannosylation (Yoshida et al., 2001; reviewed in Endo and Toda, 2003). Mutations in the *POMGnT1* gene cause muscle–eye–brain (MEB) disease, a rare autosomal recessive disorder characterized by congenital muscular dystrophy with elevated serum creatine kinase (CK) levels, severe visual failure, and gross mental retardation (Yoshida et al., 2001).

* *Corresponding author.* Tel.: +81 42 346 1720; fax: +81 42 346 1750.
E-mail address: miyagoe@ncnp.go.jp (Y. Miyagoe-Suzuki).
0925-4773/$ - see front matter © 2008 Elsevier Ireland Ltd. All rights reserved.
doi:10.1016/j.mod.2008.12.001

α-Dystroglycan (α-DG) is a heavily glycosylated glycoprotein and a well-known substrate of POMGnT1. Dystroglycan is encoded by a single gene (*DAG1*) and is cleaved into two proteins, α-dystroglycan (α-DG) and β-dystroglycan (β-DG), by posttranslational processing (Ibraghimov-Beskrovnaya et al., 1992). DGs are central components of the dystrophin–glycoprotein complex (DGC) at the sarcolemma, and α-DG was shown to serve as a cell surface receptor for laminin (Ibraghimov-Beskrovnaya et al., 1992), agrin (Gee et al., 1994; Campanelli et al., 1994), perlecan (Peng et al., 1998; Kanagawa et al., 2005), and neurexin (Sugita et al., 2001). In skeletal muscle, the laminin-α-DG linkage is thought to be critical for plasma membrane stability (recently reviewed in Kanagawa and Toda 2006). In MEB muscle, the α-DG core protein is preserved but hypo-glycosylated, and α-DG prepared from the muscle fails to bind laminin *in vitro* (Michele et al., 2002). Therefore, it is proposed that the disruption of the α-DG-laminin linkage is the main pathomechanism of dystrophic changes seen in MEB muscle.

To further elucidate the molecular pathogenesis of MEB disease, we generated *POMGnT1*-knockout mice using a gene targeting technique, and examined the mutant skeletal muscle. During our experiments, Liu et al. reported the generation of POMGnT1-deficient mice (Liu et al., 2006). The report showed severe muscle pathology, but the mechanism by which POMGnT1 deficiency causes muscle phenotype was not clearly shown. In this report, we report that POMGnT1-deficient mice show remarkably minimal signs of muscle degeneration and regeneration, but also show small muscle mass, reduced numbers of muscle fibers, and impaired muscle regeneration. POMGnT1-deficient myoblasts proliferate poorly *in vitro*. The proliferation was not improved by retrovirus vector-mediated *POMGnT1* expression in *POMGnT1*$^{-/-}$ myoblasts, suggesting that α-DG–laminin interaction *in vivo* is important for maintenance of the proliferative activity of satellite cells.

2. Results

2.1. *Inactivation of the POMGnT1 gene in mice*

We mutated the *POMGnT1* gene by replacing exon 18 with a neomycin-resistance gene in mouse ES cells (depicted in Fig. 1). Two ES clones successfully entered the germline. Although there was no evidence of embryonic lethality, more than 60% of the homozygotes died within 3 weeks of birth. Survivors were smaller than their wild-type littermates (Fig. 3A) throughout life, but most of them had a normal life span. We confirmed that the *POMGnT1*$^{-/-}$ mice completely lacked the POMGnT1 enzyme activity (Fig. 2A). A monoclonal antibody, VIA4-1, that reacts with the suger moiety of α-DG gave no signal in either *POMGnT1*$^{-/-}$ brain (Fig. 2B) or muscle (data not shown). A polyclonal antibody against α-DG core protein revealed that the *POMGnT1*$^{-/-}$ brain expresses approximately 80 kDa α-DG protein, which is much smaller than that seen in the wild-type brain (ca. 110 kDa) (Fig. 2C). We next examined whether α-DG in *POMGnT1*$^{-/-}$ brain binds laminin. Wheat germ agglutinin (WGA)-enriched brain protein from control and *POMGnT1*$^{-/-}$ mice was separated on SDS–PAGE gels, blotted onto a PVDF membrane, incubated with EHS laminin, and then bound laminin was detected by an anti-laminin antibody. α-DG in *POMGnT1*$^{-/-}$ brain failed to bind to laminin (Fig. 2D).

2.2. *POMGnT1*$^{-/-}$ *muscle shows very mild dystrophic changes*

Immunohistochemistry of cross-sections of tibialis anterior (TA) muscles showed that dystrophin and other members of the DGC complex were normally expressed at the sarcolemma of *POMGnT1*$^{-/-}$ muscle (Fig. 3 and Table 1). Laminin α2 chain was detected around POMGnT1$^{-/-}$ muscle fibers. On H.E.-stained cross-sections, surprisingly, the POMGnT1$^{-/-}$ muscle showed almost normal morphology. Central nucleation of myofibers indicates regeneration events in the past. In the TA muscles of 4-week-old wild-type mice, 0.25% of myofibers were centrally nucleated. In POMGnT1$^{-/-}$ mice, 0.28% of the myofibers had central nuclei. In contrast, ca. 40–50% of myofibers of age-matched mdx mice were centrally nucleated. Even at 24 months of age, the percentage of centrally nucleated myofibers was lower (3.6%) in POMGnT1$^{-/-}$ TA muscle, compared with age-matched wild-type TA muscle (9.0%). POMGnT1$^{-/-}$ TA muscle also lacked other signs of degeneration and regeneration. Electrophoresis of muscle extracts on glycerol SDS–PAGE gels showed no difference in MyHC isoform composition of quadriceps and gastrocnemius muscles between POMGnT1$^{-/-}$ and wild-type littermates (data not shown). In both wild-type and POMGnT1$^{-/-}$ muscle, the muscle basal lamina was normally formed (Supplementary Fig. 1). Electron microscopy also showed that the sarcomere structures are almost normal in POMGnT1$^{-/-}$ mice. We next examined the serum creatine kinase (CK) levels, an index of on-going muscle damage, in wild-type, POMGnT1$^{-/-}$, and age-matched mdx mice (Fig. 5). The serum CK levels of 5- to 20-week-old POMGnT1$^{-/-}$ mice were slightly higher (av. 586 U/L, $n = 10$) ($p < 0.05$) than those of wild-type littermates (less than 100 U/L, $n = 4$), but were much lower than those of mdx mice (more than 5000 U/L, $n = 3$, $p < 0.01$). The serum CK levels of 2-year-old POMGnT1$^{-/-}$ mice were still low (less than 300 U/L, $n = 4$).

2.3. *Repetitive muscle injury causes more fibrosis and fatty infiltration in POMGnT1*$^{-/-}$ *than in WT TA muscle*

Dystroglycans expressed on the cell membrane of satellite cells are proposed to play an important role in muscle regeneration (Cohn et al., 2002). In addition, the average size of *POMGnT1*$^{-/-}$ myofibers was smaller than those of wild-type myofibers (Fig. 4). Moreover, the number of myofibers is reduced in *POMGnT1*$^{-/-}$ skeletal muscle of neonatal and adult POMGnT1 mice, suggesting proliferation defect of *POMGnT1*$^{-/-}$ myoblasts (Fig. 4). To test the hypothesis, we damaged *POMGnT1*$^{-/-}$ TA muscle by cardiotoxin (CTX) and examined their regeneration. After single cardiotoxin injection, *POMGnT1*$^{-/-}$ muscle regenerated well like wild-type (data not shown). Next, we injected CTX into TA muscles of *POMGnT1*$^{-/-}$ and heterozygous littermates three times at intervals of 2 weeks, or 1 week interval, and examined the muscle. We summarized the results in Fig. 6. *POMGnT1*$^{-/-}$ muscle showed more fibrosis and

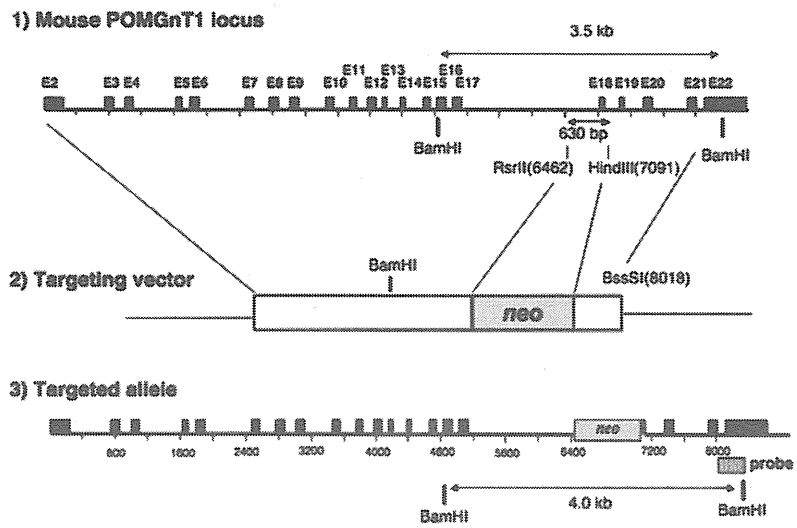

Fig. 1 – Targeted disruption of the mouse *POMGnT1* gene in embryonic stem (ES) cells. The successfully targeted allele lacks a 630 bp-genome fragment containing exon 18, and instead has a *neo* resistance gene. Recombination in ES cells was confirmed by Southern blotting with the probe shown by a shaded box. The nucleic acid numbers are from AB053221 in GenBank.

fatty infiltration, which is a sign of inefficient muscle regeneration, than *POMGnT1*$^{+/-}$ muscle. Together with reduced numbers of myofibers in muscle, the results suggest that the function of satellite cells in *POMGnT1*$^{-/-}$ skeletal muscle is impaired.

2.4. *Defective proliferative activity of POMGnT1*$^{-/-}$ *myoblasts*

We next tested activation and proliferation of satellite cells on living myofibers isolated from wild-type and *POMGnT1*$^{-/-}$

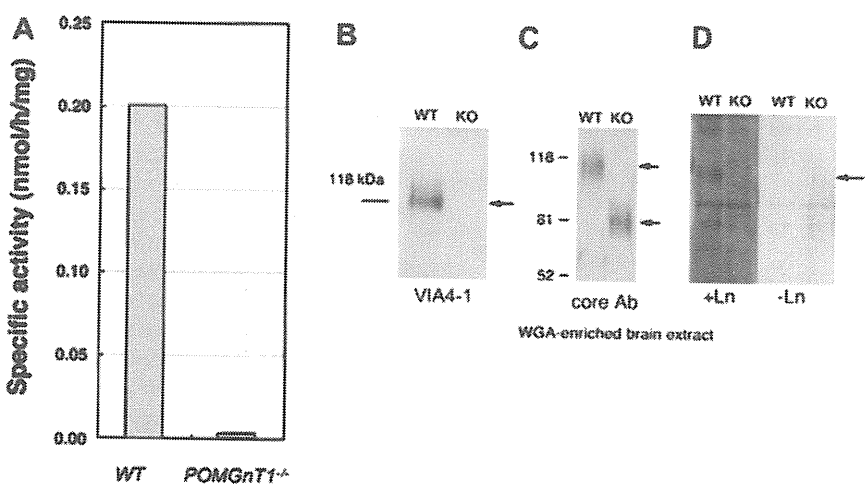

Fig. 2 – *POMGnT1*$^{-/-}$ mice show undetectable POMGnT1 enzyme activity and aberrant glycosylation of α-dystroglycan (α-DG) in *POMGnT1*$^{-/-}$ mice. (A) The amount of POMGnT1 activity is based on the amount of [^{3}H]GlcNAc transferred from UDP-GlcNAc to mannosyl peptide. The reaction product was purified by reverse-phased HPLC, and the radioactivity was measured. (B) Wheat germ agglutinin (WGA) agarose-enriched brain extracts from wild-type (WT) or *POMGnT1*$^{-/-}$ (KO) mice were resolved on a 7.5% SDS–PAGE gel, transferred to a PVDF membrane, and probed with anti-α-DG antibody, VIA4-1, which recognizes glycosylated α-DG. (C) The blot was incubated with polyclonal antibodies specific for α-DG core protein. The antibody detected ~110 kDa bands in wild-type brain extract, and 80 kDa bands in the brain extract of *POMGnT1*$^{-/-}$ mice. (D) Laminin overlay assay showing that α-DG in *POMGnT1*$^{-/-}$ brain does not bind laminin *in vitro*. +Ln, laminin was incubated with the blotted membrane. –LN, without laminin.

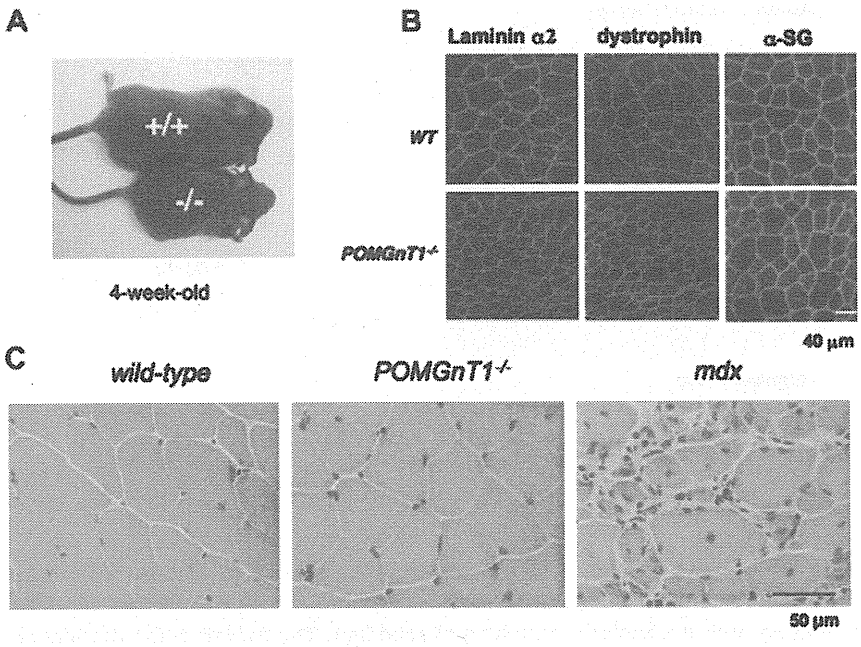

Fig. 3 – Remarkably mild dystrophic phenotypes of POMGnT1$^{-/-}$ muscle. (A) A photo of representative 4-week-old wild-type (+/+) and POMGnT1$^{-/-}$ (−/−) mice. POMGnT1$^{-/-}$ mice are smaller than wild-type littermates. (B) Immunohistochemistry of wild-type (+/+) and POMGnT1-knockout (−/−). Laminin α2 chain, dystrophin, and α-sarcoglycan are expressed normally on the sarcolemma of POMGnT1$^{-/-}$ muscle. (C) Representative H.E. staining of cross-sections of the TA muscles from POMGnT1$^{-/-}$, wild-type, and age-matched dystrophin-deficient *mdx* mice. POMGnT1$^{-/-}$ muscle shows minimal signs of degeneration and regeneration.

Table 1 – Summary of immunohistochemistry of hind-limb muscles of wild-type (WT) POMGnT1$^{-/-}$, and mdx mice.

	WT	POMGnT1$^{-/-}$	*mdx*
Laminin α2 chain	+	+	+
Dystrophin	+	+	−
α-Dystroglycan (VIA4–1)	+	−	±
Dystroglycan (core protein)	+	+	±
β-Dystropglycan	+	+	±
α-Sarcoglycan	+	+	±
α-Syntrophin	+	+	±
nNOS	+	+	±
Aquaporin 4	+	+	±
Integrin α7	+	+	++
Integrin β1	+	+	++

+, expressed; −, absent; ±, down-regulated; ++, up-regulated.

mice (Fig. 7). Three days after plating of single myofibers on Matrigel-coated 24-well plates in growth medium, the numbers of detached satellite cells (activated and proliferating satellite cells) were counted. In both extensor digitorum longus (EDL) (fast twitch muscle) and soleus (slow twitch muscle) muscles, the numbers of activated satellite cells and proliferating satellite cells (myoblasts) around the parental myofiber were more numerous in wild-type than in POMGnT1$^{-/-}$ (Fig. 7). Furthermore, wild-type satellite cells migrate a little faster than POMGnT1$^{-/-}$ satellite cells on transwells (data not shown), although the difference was little. Therefore, our results suggest that POMGnT1$^{-/-}$ satellite cells are activated more slowly or proliferate more slowly than wild-type. We next isolated satellite cells from hind limb muscles of wild-type and POMGnT1$^{-/-}$ mice by a monoclonal antibody, SM/C-2.6, and flow cytometry (Fukada et al., 2007), and examined their proliferation rate. The total yield of satellite cells per gram of POMGnT1$^{-/-}$ muscle tissue was nearly the same as those of wild-type muscle (data not shown). The percentage of Ki67-positive satellite cells (cycling cells) was less than 1% in both wild-type and POMGnT1$^{-/-}$ mice, indicating that they are in the quiescent stage (data not shown). However, after plating wild-type and POMGnT1$^{-/-}$ satellite cells onto Matrigel-coated 6-well plates at the same density, we found that POMGnT1$^{-/-}$ satellite cells grew poorly in growth medium (Fig. 7B). The timing of activation (i.e. enlargement of the cytoplasm and MyoD expression) was the same with that of wild-type satellite cells (data not shown). Next, we cultured satellite cells on Matrigel-coated 24-well-plates in growth medium, and the cells growth was evaluated by MTT assay 1, 2, 3, 4, 5, 6, and 7 days after plating (Fig. 8). The assay revealed that wild-type myoblasts proliferated more rapidly than POMGnT1$^{-/-}$ myoblasts *in vitro*. POMGnT1$^{-/-}$ myoblasts fused normally to form multinucleated myotubes in differentiation conditions like the wild-type (data not shown), and there was no significant difference in the fusion index between wild-type (45%) and POMGnT1$^{-/-}$ myoblasts (40%) ($p > 0.05$).

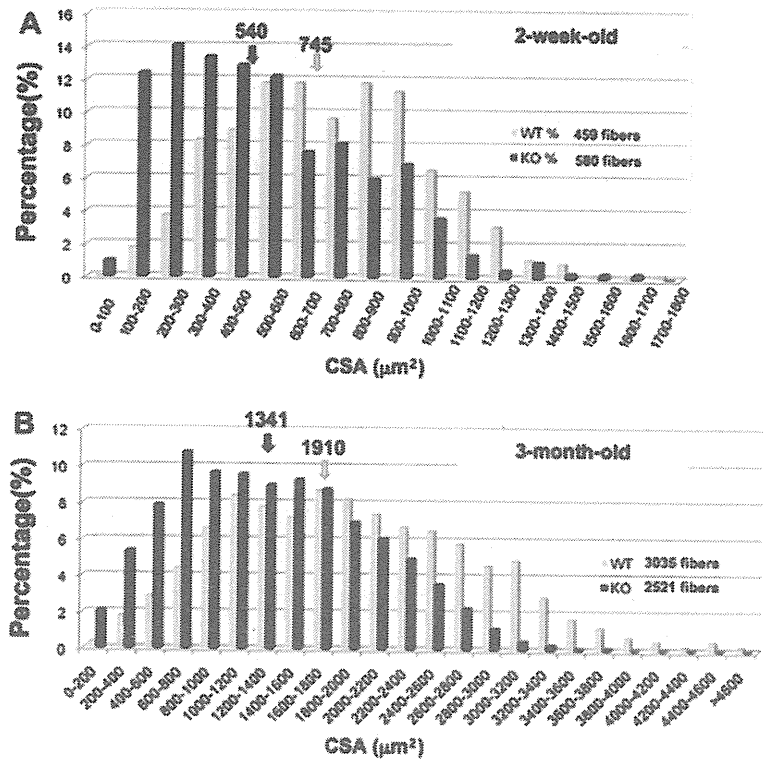

Fig. 4 – Cross-sectional area (CSA) of myofibers of *POMGnT1*$^{-/-}$ and wild-type mice. (A) A representative frequency graph of CSA of rectus femoris muscles from 2-week-old *POMGnT1*$^{-/-}$ (blue) and wild-type (light blue) littermates. The cross-sections were stained with anti-laminin α2 chain antibody. CSA of 459 *POMGnT1*$^{-/-}$ fibers and 580 wild-type fibers were measured and plotted. X-axis indicates CSA (μm²), and Y-axis indicates percentages. Arrows indicate the averages. The total number of myofibers was also reduced in *POMGnT1*$^{-/-}$ mice (4169 vs. 3510). (B) The CSA of myofibers in TA muscles from 3-month-old *POMGnT1*$^{-/-}$ (blue) and wild-type (light blue) male mice was plotted as in (A)). In (B), almost all myofibers were measured (3035 fibers in wild-type TA and 2521 fibers in *POMGnT1*$^{-/-}$ TA).

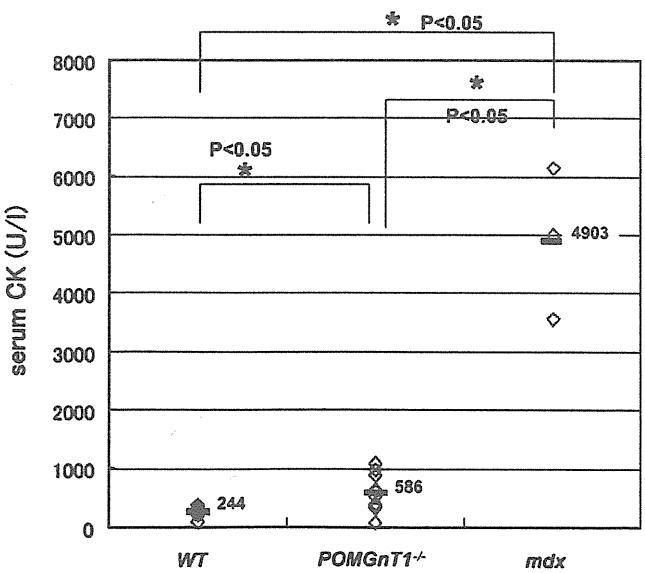

Fig. 5 – Serum CK levels of *POMGnT1*$^{-/-}$, wild-type, and *mdx* mice. Serum CK levels of 7–20 weeks old *POMGnT1*$^{-/-}$ mice (5 males and 5 females), wild-type littermates (3 males and 1 female), and three male *mdx* mice were measured and plotted on the graph with average. *$p < 0.05$.

Next, we examined whether restoration of the expression of the *POMGnT1* gene in mutant myoblasts improved their proliferation. To this end, we prepared a retrovirus vector, (pMX-POMGnT1-IRES-GFP) expressing human *POMGnT1* and GFP. The recombinant retrovirus successfully restored O-mannosyl glycosylation of α-DG (Fig. 7A), but the proliferation rate was not changed (Fig. 8B).

2.5. *Cell growth signaling in POMGnT1*$^{-/-}$ *myoblasts*

It was previously reported that enhanced expression of α7β1 integrin ameliorates the development of muscular dystrophy and extends longevity in α7BX2-*mdx/utr*$^{(-/-)}$ transgenic mice (Burkin et al., 2001; Burkin et al., 2005), suggesting that integrin compensates for the function of α-DG in skeletal muscle to some extent. Therefore, we next examined the expression of β1-integrin in wild-type and *POMGnT1*$^{-/-}$ myoblasts (Supplementary Fig. 1). Western blotting, however, showed no difference between the β1-integrin protein levels in wild-type and *POMGnT1*$^{-/-}$ myoblasts (Supplementary Fig. 1A). Furthermore, FACS analysis showed similar levels of β1 integrin expression on the surfaces of myoblasts (Supplementary Fig. 1B). We then examined the activation levels of Akt and GSK-3β, both of which are involved in the

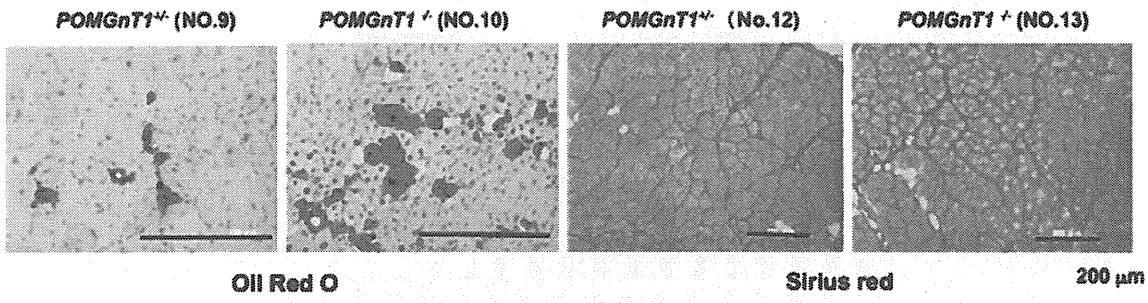

	genotype	sex	age	CTX interval(x3)	Fatty infiltration	Fibrosis
1	+/-	F	3M	2w	-	-
2	+/-	F	3M	2w	-	-
3	+/-	F	3M	2w	-→+	-→
4	+/-	F	3M	2w	+	-→
5	-/-	M	3M	2w	+	-→
6	-/-	F	3M	2w	++	-→
7	+/-	F	11M	1w	+	+
8	-/-	F	8.5M	1w	+	++
9	+/-	F	8.5M	1w	+	-→
10	-/-	F	8.5M	1w	+→++	+→++
11	+/-	M	8.5M	1w	+	+
12	+/-	M	8.5M	1w	++	+
13	-/-	M	8.5M	1w	++	++

Fig. 6 – Impaired muscle regeneration of *POMGnT1*$^{-/-}$ mice. upper panel: representative Oil red O-stained or Sirius red-stained cross-sections of TA muscles of *POMGnT1*$^{-/-}$(−/−) and *POMGnT1*$^{+/-}$ (+/−) mice after three rounds of degeneration/regeneration evoked by cardiotoxin injection. One week after the last CTX injection, TA muscles were dissected, sectioned by a cryostat, fixed, and stained. lower table: Summary of fatty infiltration and fibrosis in regenerated muscles. CTX was injected into TA muscles three times with 2 weeks interval (2w) or 1 week interval (1w). The age at the first injection was shown. (−), well regenerated with minimal changes. (−→+), sporadic fatty regeneration or slight fibrosis between fibers. (+), mild fatty infiltration or mild fibrosis. (++), dense fatty infiltration or extensive fibrosis. F, female; M, male.

regulation of cell survival and proliferation. The levels of phosphorylation of these two kinases in *POMGnT1*$^{-/-}$ myoblasts were similar with those in wild-type myoblasts (Supplementary Fig. 1C). Consistent with these observations, TUNEL assay indicated that apoptosis is rare both in *POMGnT1*$^{-/-}$ and wild-type muscles (data not shown).

3. Discussion

In this study, we showed that in spite of mild muscle degeneration, the *POMGnT1*$^{-/-}$ satellite cells have much lower proliferative activity than wild-type satellite cells. The defect was not recovered by restoration of normal glycosylation of α-DG in mutant satellite cells. Together with the reduced sizes and the reduced numbers of myofibers of neonatal and adult *POMGnT1*$^{-/-}$ mice, these observations suggest that deficiency of POMGnT1 enzymatic activity impairs the functions of satellite cells.

3.1. *Two mouse models of muscle–eye–brain (MEB) disease*

Our *POMGnT1*$^{-/-}$ mice are the second mouse model of MEB disease. The first one was generated by gene trapping with a retroviral vector inserted into the second exon of the mouse *POMGnT1* locus (Liu et al., 2006). As described in the literature, the phenotype is similar to ours with some differences. Our model shows much milder muscle phenotypes than the previously reported model, but also shows much a lower survival rate in the postnatal stage than the first model does. This would be due to more severe developmental abnormalities of the central nervous system of our mouse model, including disruption of the glia limitans, abnormal migration of neurons, and reactive gliosis in the cerebral cortex (manuscript in preparation), although these are also observed in the first model (Yang et al., 2007; Hu et al., 2007).

Mutation of the *POMGnT1* gene is the cause of muscle–eye–brain disease (MEB) (Yoshida et al., 2001), which is characterized by severe congenital muscular dystrophy (Voit and Tome, 2004). Although glycosylation of α-DG was completely perturbed in our model, the *POMGnT1*$^{-/-}$ muscle showed only marginal pathological changes. Furthermore, *POMGnT1*$^{-/-}$ muscle showed normally formed muscle basal lamina on EM. These observations are in sharp contrast to the condition in humans. One possibility is that in the mouse, molecules other than α-DG are involved in the linkage of the sarcolemma with the extracellular matrix proteins, stabilizing the plasma membrane. As a candidate molecule, we examined β1-integrin expression in *POMGnT1*$^{-/-}$ muscle, but found that the level was not up-regulated. Therefore, the mechanism that explains this discrepancy remains to be clarified in a future study.

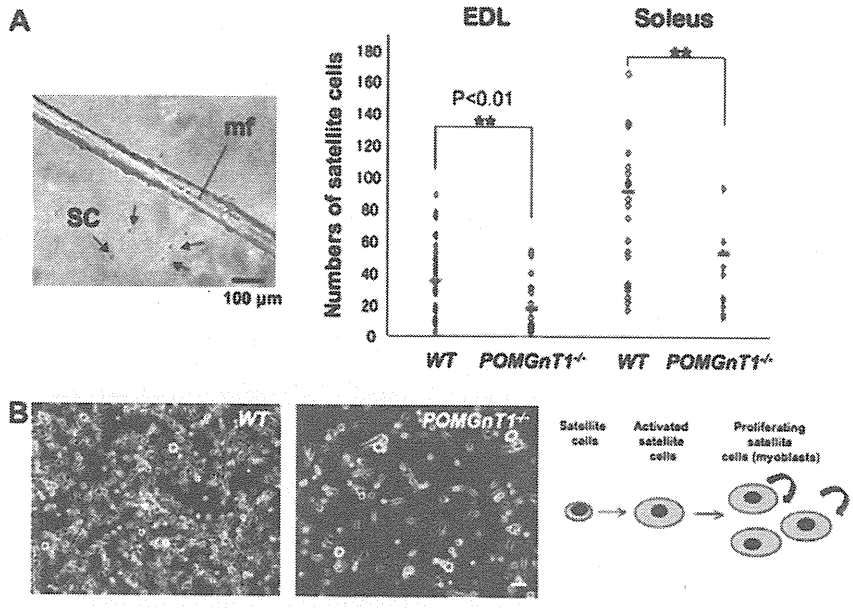

Fig. 7 – Activation and proliferation of satellite cells from WT and *POMGnT1*$^{-/-}$ mice. (A) Isolated myofibers were plated on Matrigel-coated 24 well-plates at one myofiber per well. Three days later, activated satellite cells (SC, arrows) around the parental fiber (mf) were counted and plotted. Small horizontal bars indicate the average number of activated/proliferating satellite cells originating from a myofiber from three independent experiments. Student's *t*-test. $^{**}p < 0.01$ (wild-type vs. *POMGnT1*$^{-/-}$ mice). (B) Satellite cells from *WT* and *POMGnT1*$^{-/-}$ mice 7 days after plating onto Matrigel-coated 24-well-plates at 2.5×10^3 cells/well. Scale bar, 100 μm.

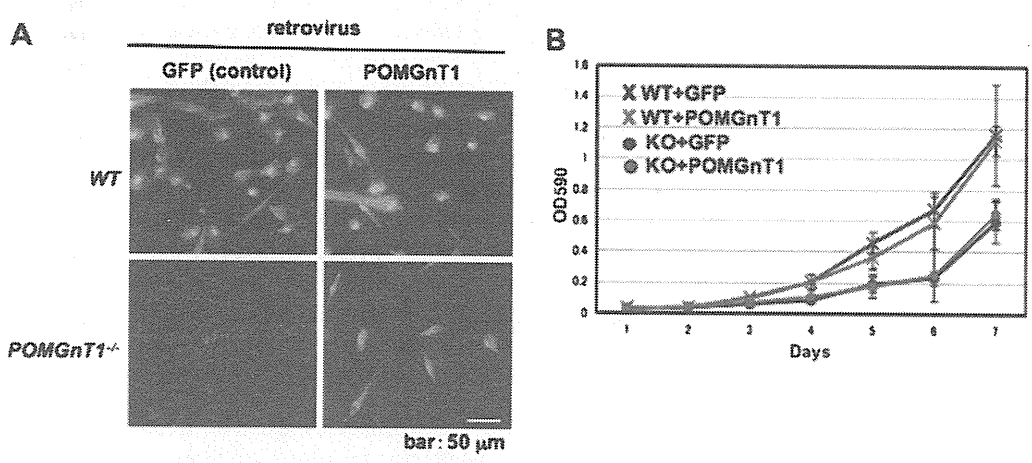

Fig. 8 – Restoration of POMGnT1 expression in *POMGnT1*$^{-/-}$ myoblasts does not improve proliferation of cells. (A) Wild-type (WT) and *POMGnT1*$^{-/-}$ myoblasts were transduced with a retrovirus expressing both POMGnT1 and GFP (POMGnT1) or only GFP (GFP, control), and the FACS-purified transduced cells were stained with anti-glycosylated α-DG monoclonal antibody (VIA4-1; red) and DAPI (Nucleus, blue). Note that the glycosylation of α-DG in *POMGnT1*$^{-/-}$ myoblasts was completely recovered by a retrovirus vector expressing POMGnT1. (B) MTT assay of wild-type (WT) and *POMGnT1*$^{-/-}$ myoblasts after infection with retrovirus vectors. Impaired proliferation of *POMGnT1*$^{-/-}$ myoblasts was not recovered by retrovirus-mediated expression of *POMGnT1*. Representative data of three independent experiments are shown.

3.2. *Null mutation in POMGnT1 reduces proliferative activity of muscle satellite cells*

POMGnT1$^{-/-}$ myoblasts proliferate poorly *in vitro*. This observation suggested that the proliferation of myoblasts is stimulated by growth signals *via* laminin-α-DG interaction. However, retrovirus vector-mediated gene transfer of the *POMGnT1* gene, which successfully restored O-mannosyl glycosylation of α-DG, did not restore the proliferation activity of the *POMGnT1*$^{-/-}$ myoblasts. DMD myoblasts proliferate poorly and quickly reach senescence. The impaired proliferation activity has been ascribed to repeated activation of

satellite cells due to repetitive cycles of muscle degeneration and regeneration (Blau et al., 1983). In contrast, *POMGnT1*$^{-/-}$ muscle lacks signs of active regeneration. Therefore, the reduced proliferation activity of *POMGnT1*$^{-/-}$ mouse myoblasts is not likely due to excessive cell division of satellite cells. Rather, it is likely that α-DG-laminin interaction in the niche, i.e. beneath the basal lamina of skeletal muscle myofibers, is important for maintenance of proliferative activity of satellite cells. However, the possibility that POMGnT1-deficiency causes aberrant glycosylation of molecules other than α-DG should be also tested.

Our results also suggested that the lack of α-DG-laminin interaction resulted in reduced numbers of muscle fibers (hypoplasia). Importantly, we found that myofibers of older *POMGnT1*$^{-/-}$ mice tend to be hypertrophied (Supplementary Fig. 2). *POMGnT1*$^{-/-}$ muscle might compensate the muscle power by hypertrophy of the myofibers. This is consistent with our observation that *POMGnT1*$^{-/-}$ muscle increases its mass in an overload model (unpublished data). Importantly, recent studies suggest that this process is satellite cell-independent (Sandri M., 2008).

Recently, Liu et al. showed that over-expression of integrin α7β1 in C2C12 myoblasts promoted proliferation of the cells (Liu et al., 2008). Importantly, however, we did not observe up-regulation of integrin α7β1 expression in *POMGnT1*$^{-/-}$ satellite cells. These observations suggest that dystroglycans and integrins have distinct roles in the regulation of muscle satellite cells.

In summary, we generated *POMGnT1*-null mice. The mice showed low serum creatine kinase levels and minimal signs of muscle degeneration and regeneration. Nonetheless, *POMGnT1*$^{-/-}$ muscle showed the reduction in the size and the number of myofibers. Furthermore, repeated injection of cardiotoxin showed impaired muscle regeneration in *POMGnT1*$^{-/-}$ mice. *POMGnT1*$^{-/-}$ myoblasts proliferated poorly *in vitro*. Over-expression of protein restored glycosylation of α-DG, but did not improve the proliferation of *POMGnT1*$^{-/-}$ myoblasts at all. Collectively, our results suggest that POMGnT1 enzymatic activity is important for maintenance of the proliferative activity of satellite cells *in vivo*.

4. Experimental procedures

4.1. *Generation of POMGnT1*$^{-/-}$ *mice*

The targeting strategy in ES cells is depicted in Fig. 1. Genomic DNA (8.6 kb) covering almost the entire *POMGnT1* gene was isolated from 129/SvJ mice by using two specific primers: m1F2 primer, 5′-gat tcc tga agt cat gga ctg gc-3′ and m1B5, 5′-tct aaa ggt ctc tgt gtg agt ctg tca g-3′. The PCR product was then cloned into a TOPO TA cloning vector (Invitrogen, Carlsbad, CA) and sequenced (AB053221). To construct the targeting vector, a 630-bp RsrII-Hind III fragment, containing exon18 was replaced with a *neo* expression cassette (Stratagene) (Fig. 1). Electroporation and screening of ES cells (129Svev origin) were performed by Ingenious Targeting Laboratory, Inc. (Stony Brook, NY). Homologous recombination in ES cells was confirmed by Southern blotting. Two independent positive ES clones were injected into C57BL/6 blastocysts, which gave rise to offspring carrying the mutated allele. Genotyping of the mice was done by PCR. One primer set is designed to amplify exon 18: F2, 5′-cag cag ttt cct tcc ttc taa ccc-3′ and B4, 5′-att tgg tct ggt ccc ttg gct c-3′ (278 bp). *Neo* primers were used to amplify the *neo* resistance gene, and thereby detect the mutant allele: neo-F, 5′-agg cta ttc ggc tat gac tgg g-3′, and neo-R, 5′-tac ttt ctc ggc agg agc aag gtg-3′ (288 bp). Dystrophin-deficient *mdx* mice of C57BL/6 genetic background were provided by T. Sasaoka at the National Institute for Basic Biology, Japan. The Experimental Animal Care and Use Committee of the National Institute of Neuroscience approved all experimental protocols.

4.2. *POMGnT1 enzymatic activity*

Brains were obtained from 8-week-old mice and homogenized with nine volumes (weight/volume) of 10 mM Tris–HCl, pH 7.4, 1 mM EDTA, and 250 mM sucrose. After centrifugation at 900*g* for 10 min, the supernatant was subjected to ultracentrifugation at 100,000*g* for 1 h. The precipitates were used as the microsomal membrane fraction. The protein concentration was determined by BCA assay (Pierce, Rockford, IL). The enzymatic activity assay measured the amount of [^{3}H]GlcNAc transferred to a mannosyl peptide (Akasaka-Manya et al., 2004). Briefly, a reaction mixture containing 140 mM Mes buffer (pH 7.0), 1 mM UDP-[^{3}H]GlcNAc (80,000 dpm/nmol, PerkinElmer, Inc., Wellesley, MA), 2 mM mannosyl peptide (Ac-Ala-Ala-Pro-Thr-(Man)-Pro-Val-Ala-Ala-Pro-NH_2), 10 mM $MnCl_2$, 2% Triton X-100, 5 mM AMP, 200 mM GlcNAc, 10% glycerol, and 100 μg of microsomal membrane fraction was incubated at 37 °C for 1 h. After boiling for 3 min, the mixture was analyzed by reverse phase HPLC using a Wakopak 5C18-200 column (4.6 × 250 mm, Wako Pure Chemical Industries, Osaka, Japan). The gradient solvents were aqueous 0.1% trifluoroacetic acid (solvent A) and acetonitrile containing 0.1% trifluoroacetic acid (solvent B). The mobile phase consisted of 100% A for 10 min and then a linear gradient to 75% A:25% B over 25 min. Peptide separation was monitored at 214 nm, and the radioactivity of each fraction (1 ml) was measured using a liquid scintillation counter.

4.3. *Antibodies*

All antibodies used in Western blotting, immunohistochemistry, and FACS are listed in Supplementary Table 1.

4.4. *Histology and immunohistochemical analysis*

Muscle cryosections (6–10 μm) were stained with hematoxylin and eosin (H&E), or treated with 0.1% Triton X-100, blocked with 5% goat serum/1% BSA in PBS, then incubated with primary antibodies (Supplementary Table 1) at 4 °C overnight. After washing with PBS, specimens were incubated with a secondary antibody labeled with Alexa Fluor 488 or Alexa Fluor 568 (1:200–400 dilution; Molecular Probes) at RT for 1 h, counterstained with TOTO-3 (1:5000; Molecular Probes), and then mounted in Vectashield (Vector). The images were recorded using a confocal laser scanning microscope system TCSSP™ (Leica). For fiber size measurement, cross-sections of muscle were stained with anti-laminin α2

antibody and recorded and quantified by a digital microscope, BIOREVO (http://www.biorevo.jp; KEYENCE, Osaka, Japan).

4.5. Western blotting

Western blotting was performed as previously described (Hosaka et al., 2002). In brief, 20 μg of muscle proteins were separated on 7.5% SDS–PAGE gels and transferred to a PVDF membrane (Millipore, Bedford, MA). After incubation with primary antibodies (Supplementary Table 1), the membranes were incubated in HRP-labeled secondary antibodies (1:5000 dilution) (Amersham Biosciences, UK). The signals were detected by using an ECL plus Western Blotting Detection System (GE Healthcare, Buckinghamshire, UK).

4.6. Laminin blot overlay assay

An overlay assay was performed as described by Moore et al. (2002). In brief, WGA-enriched homogenates were prepared from wild-type and *POMGnT1*$^{-/-}$ brains, separated on SDS–PAGE gels, blotted onto a PDVF membrane, and incubated with mouse EHS laminin (Trevigen, Gaithersburg, MD, USA). Bound laminin was probed with anti-laminin antibody (Sigma, St. Louis, MO) and ECL system (GE Healthcare, Buckinghamshire, UK).

4.7. Single fiber preparation and culture

Single fibers were prepared from extensor digitorum longus (EDL) and soleus muscles of wild-type and *POMGnT1*$^{-/-}$ mice as described by Rosenblatt et al. (1995). Each fiber was plated onto Matrigel (BD Biosciences, Bedford, MA)-coated 24-well plates and cultured in growth medium for 3 days. Then, the number of cells around the parental fiber was counted.

4.8. Isolation of satellite cells, proliferation assay, and fusion index

Satellite cells were prepared from wild-type and *POMGnT1*$^{-/-}$ mice by FACS as previously described (Fukada et al., 2007). Sorted cells were plated on Matrigel-coated 24-well-plates at a density of 1×10^4 cells/well in a growth medium, DMEM (High glucose; Wako, Osaka), supplemented with 20% fetal bovine serum (Equitech-bio, Inc., Kerville, TX), human recombinant bFGF (2.5 ng/ml) (Invitrogen), recombinant mouse HGF (25 ng/ml) (R&D Systems, Minneapolis, MN), and heparin (5 μg/ml) (Sigma). For the MTT assay, 100 μl of 0.5% MTT (3-(4,5-dimethylthiazol-2-yl)-2,5-diphenyltetrazolium bromide) (Dojindo, Kumamoto, Japan) was added to the culture at each time point, and after 4 h incubation, the cells were collected in 1 ml of acid isopropanol solution. OD_{590} was measured and plotted. After reaching 70% confluency, the cells were induced to differentiate into myotubes by low-serum medium (5% horse serum/DMEM), and 18 h later, the cells were fixed, stained with anti-sarcomeric α-actinin antibody and DAPI (nuclei). Fusion index was calculated as (the numbers of nuclei in the myotubes/total nuclei) × 100%.

4.9. Production of retrovirus vectors

pMXs-IG (Kitamura et al., 2003) was kindly provided by T.Kitamura at Tokyo University. Human POMGnT1 cDNA, which has an Xpress epitope and a His-tag at the N-terminal (Akasaka-Manya et al., 2004), was cloned into the multi-cloning site upstream of IRES-GFP of the vector. Vector particles were produced by transfection of the vector plasmid into PLAT-E packaging cells (Kitamura et al., 2003). Proliferating satellite cells (myoblasts) were incubated with the viral vectors overnight and 4 days later, successfully transduced GFP-positive cells were collected by FACS, and the proliferation rate was evaluated by MTT assay.

4.10. Electron microscopy

Mice were perfused transcardially with a solution of 2% paraformaldehyde and 2.5% glutaraldehyde in PBS under deep pentobarbital anesthesia. The anterior tibial muscles were excised, embedded in 3% agarose, and sections (70 μm in thickness) were prepared on a Vibratome. Sections were fixed in OsO_4, ehydrated, and embedded in Cartepoxy resin. Ultrathin sections were prepared, stained with lead citrate and uranyl acetate, and observed under a Hitachi H-7000 transmission electron microscope.

4.11. Measurement of serum creatine kinase (CK)

Blood samples were obtained from the tail vein or directly from the heart at sacrifice. Serum CK level was measured by colorimetric assay using an FDC3500 clinical biochemistry autoanalyzer (FujiFilm Medical Co., Tokyo, Japan).

4.12. Cardiotoxin (CTX) injection

To induce muscle regeneration, CTX (10 μmol/L in saline; Sigma, St. Louis, MO) was injected into the tibialis anterior (TA) muscles three times at indicated intervals. The muscle cross-sections were stained with Oil red O (Muto Pure Chemicals Co., Ltd., Tokyo, Japan) to detect lipid droplets, or with Sirius red F3B (Sigma Chemical Co., St. Louis, MO) in saturated picric acid to stain collagen fibers.

Acknowledgments

This work was supported by Health Science Research Grants for Research on the Human Genome and Gene Therapy (H16-genome-003). For research on Phychiatric and Neurological Diseases and Mental Health (H18-kokoro-019; H20-016) from the Japanese Ministry of Health, Labor and Welfare, and Grants-in-Aid for Scientific Research (18590392) from the Japanese Ministry of Education, Culture, Sports, Science and Technology.

Appendix A. Supplementary data

Supplementary data associated with this article can be found, in the online version, at doi:10.1016/j.mod.2008.12.001.

REFERENCES

Akasaka-Manya, K., Manya, H., Kobayashi, K., Toda, T., Endo, T., 2004. Structure–function analysis of human protein O-linked mannose beta1,2-N-acetylglucosaminyltransferase 1, POMGnT1. Biochem. Biophys. Res. Commun. 320, 39–44.

Blau, H.M., Webster, C., Pavlath, G.K., 1983. Defective myoblasts identified in Duchenne muscular dystrophy. Proc. Natl. Acad. Sci. USA 80, 4856–4860.

Burkin, D.J., Wallace, G.Q., Milner, D.J., Chaney, E.J., Mulligan, J.A., Kaufman, S.J., 2005. Transgenic expression of α7β1 integrin maintains muscle integrity, increases regenerative capacity, promotes hypertrophy, and reduces cardiomyopathy in dystrophic mice. Am. J. Pathol. 166, 253–263.

Burkin, D.J., Wallace, G.Q., Nicol, K.J., Kaufman, D.J., Kaufman, S.J., 2001. Enhanced expression of the alpha 7 beta 1 integrin reduces muscular dystrophy and restores viability in dystrophic mice. J. Cell Biol. 152, 1207–1218.

Campanelli, J.T., Roberds, S.L., Campbell, K.P., Scheller, R.H., 1994. A role for dystrophin-associated glycoproteins and utrophin in agrin-induced AChR clustering. Cell 77, 663–674.

Cohn, R.D., Henry, M.D., Michele, D.E., Barresi, R., Saito, F., Moore, S.A., Flanagan, J.D., Skwarchuk, M.W., Robbins, M.E., Mendell, J.R., Williamson, R.A., Campbell, K.P., 2002. Disruption of DAG1 in differentiated skeletal muscle reveals a role for dystroglycan in muscle regeneration. Cell 110, 639–648.

Endo, T., Toda, T., 2003. Glycosylation in congenital muscular dystrophies. Biol. Pharm. Bull. 26, 1641–1647.

Fukada, S., Uezumi, A., Ikemoto, M., Masuda, S., Segawa, M., Tanimura, N., Yamamoto, H., Miyagoe-Suzuki, Y., Takeda, S., 2007. Molecular signature of quiescent satellite cells in adult skeletal muscle. Stem Cells 25, 2448–2459.

Gee, S.H., Montanaro, F., Lindenbaum, M.H., Carbonetto, S., 1994. Dystroglycan-alpha, a dystrophin-associated glycoprotein, is a functional agrin receptor. Cell 77, 675–686.

Hosaka, Y., Yokota, T., Miyagoe-Suzuki, Y., Yuasa, K., Imamura, M., Matsuda, R., Ikemoto, T., Kameya, S., Takeda, S., 2002. Alpha1-syntrophin-deficient skeletal muscle exhibits hypertrophy and aberrant formation of neuromuscular junctions during regeneration. J. Cell Biol. 158, 1097–1107.

Hu, H., Yang, Y., Eade, A., Xiong, Y., Qi, Y., 2007. Breaches of the pial basement membrane and disappearance of the glia limitans during development underlie the cortical lamination defect in the mouse model of muscle–eye–brain disease. J. Comp. Neurol. 502, 168–183.

Ibraghimov-Beskrovnaya, O., Ervasti, J.M., Leveille, C.J., Slaughter, C.A., Sernett, S.W., Campbell, K.P., 1992. Primary structure of dystrophin-associated glycoproteins linking dystrophin to the extracellular matrix. Nature 355, 696–702.

Kanagawa, M., Michele, D.E., Satz, J.S., Barresi, R., Kusano, H., Sasaki, T., Timpl, R., Henry, M.D., Campbell, K.P., 2005. Disruption of perlecan binding and matrix assembly by post-translational or genetic disruption of dystroglycan function. FEBS Lett. 579, 4792–4796.

Kanagawa, M., Toda, T., 2006. The genetic and molecular basis of muscular dystrophy: roles of cell–matrix linkage in the pathogenesis. J. Hum. Genet. 51, 915–926.

Kitamura, T., Koshino, Y., Shibata, F., Oki, T., Nakajima, H., Nosaka, T., Kumagai, H., 2003. Retrovirus-mediated gene transfer and expression cloning: powerful tools in functional genomics. Exp. Hematol. 31, 1007–1014.

Liu, J., Ball, S.L., Yang, Y., Mei, P., Zhang, L., Shi, H., Kaminski, H.J., Lemmon, V.P., Hu, H., 2006. A genetic model for muscle–eye–brain disease in mice lacking protein O-mannose 1,2-N-acetylglucosaminyltransferase (POMGnT1). Mech. Dev. 123, 228–240.

Liu, J., Burkin, D.J., Kaufman, S.J., 2008. Increasing alpha 7 beta 1-integrin promotes muscle cell proliferation, adhesion, and resistance to apoptosis without changing gene expression. Am. J. Physiol. Cell Physiol. 294, C627–C640.

Michele, D.E., Barresi, R., Kanagawa, M., Saito, F., Cohn, R.D., Satz, J.S., Dollar, J., Nishino, I., Kelley, R.I., Somer, H., Straub, V., Mathews, K.D., Moore, S.A., Campbell, K.P., 2002. Post-translational disruption of dystroglycan–ligand interactions in congenital muscular dystrophies. Nature 418, 417–422.

Moore, S.A., Saito, F., Chen, J., Michele, D.E., Henry, M.D., Messing, A., Cohn, R.D., Ross-Barta, S.E., Westra, S., Williamson, R.A., Hoshi, T., Campbell, K.P., 2002. Deletion of brain dystroglycan recapitulates aspects of congenital muscular dystrophy. Nature 418, 422–425.

Peng, H.B., Ali, A.A., Daggett, D.F., Rauvala, H., Hassell, J.R., Smalheiser, N.R., 1998. The relationship between perlecan and dystroglycan and its implication in the formation of the neuromuscular junction. Cell Adhes. Commun. 5, 475–89.

Rosenblatt, J.D., Lunt, A.I., Parry, D.J., Partridge, T.A., 1995. Culturing satellite cells from living single muscle fiber explants. In Vitro Cell Dev. Biol. Anim. 31, 773–779.

Sandri M., 2008. Signaling in muscle atrophy and hypertrophy. Physiology (Bethesda) 23, 160–170.

Sugita, S., Saito, F., Tang, J., Satz, J., Campbell, K., Südhof, T.C., 2001. A stoichiometric complex of neurexins and dystroglycan in brain. J. Cell Biol. 154, 435–445.

Voit, T., Tome, F.S., 2004. The congenital muscular dystrophies. In: Engel, A.G., Franzini-Armstrong, C. (Eds.), Myology. McGraw-Hill, New York, pp. 1203–1238.

Yang, Y., Zhang, P., Xiong, Y., Li, X., Qi, Y., Hu, H., 2007. Ectopia of meningeal fibroblasts and reactive gliosis in the cerebral cortex of the mouse model of muscle–eye–brain disease. J. Comp. Neurol. 505, 459–477.

Yoshida, A., Kobayashi, K., Manya, H., Taniguchi, K., Kano, H., Mizuno, M., Inazu, T., Mitsuhashi, H., Takahashi, S., Takeuchi, M., Herrmann, R., Straub, V., Talim, B., Voit, T., Topaloglu, H., Toda, T., Endo, T., 2001. Muscular dystrophy and neuronal migration disorder caused by mutations in a glycosyltransferase, POMGnT1. Dev. Cell 1, 717–724.

A Renaissance for Antisense Oligonucleotide Drugs in Neurology

Exon Skipping Breaks New Ground

Toshifumi Yokota, PhD; Shin'ichi Takeda, MD, PhD; Qi-Long Lu, MD, PhD; Terence A. Partridge, PhD; Akinori Nakamura, MD, PhD; Eric P. Hoffman, PhD

Antisense oligonucleotides are short nucleic acid sequences designed for use as small-molecule drugs. They recognize and bind to specific messenger RNA (mRNA) or pre-mRNA sequences to create small double-stranded regions of the target mRNA that alter mRNA splicing patterns or inhibit protein translation. Antisense approaches have been actively pursued as a form of molecular medicine for more than 20 years, but only one has been translated to a marketed drug (intraocular human immunodeficiency virus treatment). Two recent advances foreshadow a change in clinical applications of antisense strategies. First is the development of synthetic DNA analogues that show outstanding stability and sequence specificity yet little or no binding to modulator proteins. Second is the publication of impressive preclinical and clinical data using antisense in an exon-skipping strategy to increase dystrophin production in Duchenne muscular dystrophy. As long-standing barriers are successfully circumvented, attention turns toward scale-up of production, long-term toxicity studies, and the challenges to traditional drug regulatory attitudes presented by tightly targeted sequence-specific drugs.

Arch Neurol. 2009;66(1):32-38

With the advent of recombinant DNA in the 1970s, it was soon realized that bacteria possess a form of regulatory machinery where small RNA transcripts can bind (hybridize) to other target RNAs and inhibit the translation of these targets.[1] These antisense RNAs were subsequently recognized as natural translational regulation mechanisms in plants and higher organisms.[2] More recently, a specialized form of antisense transcript was found to be a cellular defense mechanism against invading messenger RNAs (mRNAs) (viruses), and this has been harnessed as a popular method to "knock down" specific mRNA transcripts in cultured cell models (short interfering RNAs).[3]

Attention soon shifted toward development of antisense molecules as a form of small-molecule drug (antisense oligonucleotide [AO]). The approach was intuitive: one needs simply to chemically synthesize short pieces of DNA of about 20 bases, where a specific complementary sequence is designed to hybridize with a desired target mRNA. Such designer AO drugs should show very high specificity and selectivity for binding only the desired target RNA sequence of nucleotides that is predicted by base pairing. Beginning in the mid-1980s, this approach was put to the test in model systems and was shown to work quite well in shutting down the production of the target (undesired) protein.[4] Isis Pharmaceuticals, Inc, Carlsbad, California, a company focused on clinical applications of AOs, was incorporated in 1989. Additional companies focusing on AO approaches soon followed.

Despite early promise, uses of AOs as small-molecule drugs have been painfully slow to enter the market and standard of care. Indeed, only a single AO drug has been approved by the Food and Drug

Author Affiliations: Research Center for Genetic Medicine, Children's National Medical Center, Washington, DC (Drs Yokota, Partridge, and Hoffman); Department of Molecular Medicine, National Institutes for Neuroscience, Tokyo, Japan (Drs Takeda and Nakamura); and McColl-Lockwood Laboratory for Muscular Dystrophy Research, Neuromuscular/ALS Center, Carolinas Medical Center, Charlotte, North Carolina (Dr Lu).

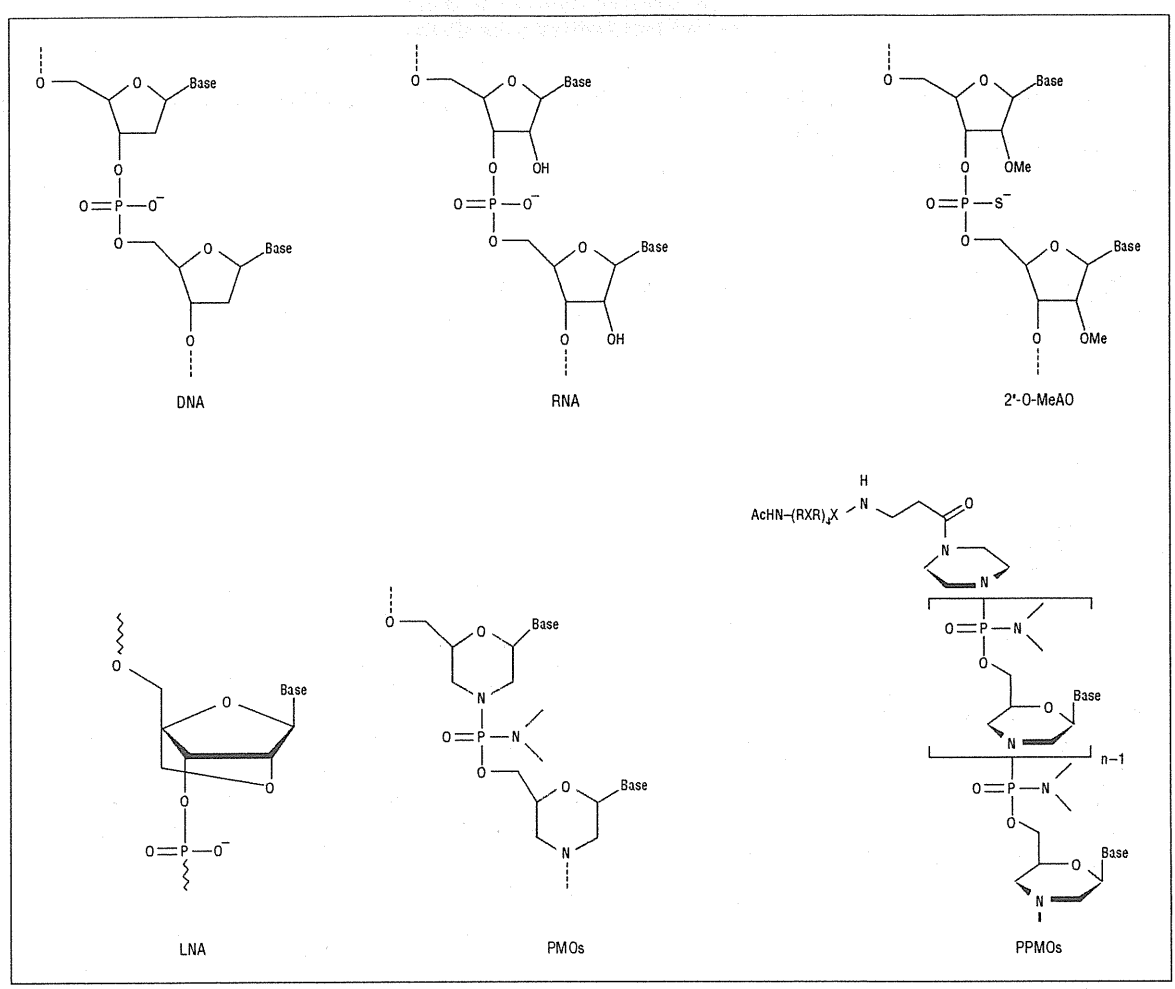

Figure 1. Comparison of chemistries used for the exon-skipping approach. Examples of artificially developed antisense oligomers such as 2′-O-methylated antisense oligonucleotides (2′-O-MeAO) (phosphorothioate), locked nucleic acid (LNA), phosphorodiamidate morpholino oligomers (PMOs), and peptide-tagged PMOs (PPMOs) are shown for comparison with DNA and RNA.

Administration (FDA), fomivirsen sodium (Vitravene; Isis Pharmaceuticals, Inc) delivered by intravitreous injection to inhibit cytomegalovirus retinitis in AIDS. Vitravene was approved in 1998 and there have been no subsequent successful approvals in the ensuing 10 years.

What has slowed the progress of AO drugs into the clinical arena, and why may this be changing?

There have been 2 major hurdles: off-target toxic effects and potency or delivery. Regarding toxic effects, most organisms do not take kindly to covert infiltration by foreign DNA or RNA. Indeed, all species have quite effective mechanisms to destroy foreign DNA and RNA as they are more likely than not to be viruses or other undesirable organisms. In addition, many of the clinical trials testing AO drugs have seen evidence of activation of the complement cascade, and this has been a key concern of the FDA. Delivery has also been a consistent problem. Because the target RNAs are always intracellular, it is imperative for the AO drug to achieve intracellular concentrations sufficient to enable it to bind and modulate the target RNA to a significant extent. The fact that AOs typically do not easily cross the lipid bilayers that bound the cell so as to achieve sufficient intracellular potency via systemic (intravenous) delivery has been problematic.

Recent developments are achieving success in overcoming both hurdles. Analogues of nucleic acid have been designed and synthesized in which the ribose backbone of RNA and DNA is replaced with different chemistries (**Figure 1**). Two are particularly promising: one uses a morpholino backbone (phosphorodiamidate morpholino oligomer [PMO]; AVI BioPharma, Portland, Oregon), and the second uses a locked nucleic acid backbone (Enzon Pharmaceuticals, Inc, Bridgewater, New Jersey). These new backbones are designed to maintain the molecular distance between bases (G, A, T/U, and C), enabling highly sequence-specific base pairing to the target RNA that is stronger in the case of PMO and locked nucleic acid drugs than DNA or RNA AOs. Equally important, these backbones are so dissimilar from the DNA and RNA ribose phosphodiester backbone that they are not recognized by most or any DNA and RNA binding proteins or degrading enzymes, thereby enhancing their stability and avoiding many or all off-target toxic effects.

The second major barrier has been achieving sufficient intracellular concentrations (delivery). One successful approach is to take advantage of preexisting holes in the plasma membrane of the target cell. Infecting viruses breach the cell membrane during the process of infection and appear to bring along AO drugs in the process. As such, AOs have been quite successful in blocking downstream viral replication within cells, and PMO drugs are showing impressive promise as antiviral antidotes.[5] Another preexisting hole is found in muscle cells lacking dystrophin (Duchenne muscular dystrophy [DMD]).[6] The unstable plasma membrane of myofibers appears to allow the AO to leak into the cell.[7] An additional approach is to modify the AO drugs with cell delivery moieties, chemical adducts that penetrate the cell membrane. One example is the addition of arginine-rich peptides to one end of the AO drug (peptide-tagged PMO) (Figure 1).

From these advances has sprung a resurgence of interest in AO drugs for treatment of genetic disease, cancer, and infectious disease. The purpose of most applications is to knock down a target RNA so that it makes less of the deleterious protein product (eg, tumor growth factor β or hypoxia-inducible factor 1α in cancer cells, viral mRNAs, or dominant gain-of-function toxic proteins in inherited neurological disease). However, the disorder that may be most advanced in such applications is DMD. Here the AOs are used for a quite different objective than for previous applications; explicitly, AOs in DMD are designed to restore function to the target mRNA and protein rather than block it. The remainder of this review focuses on this application.

RATIONALE AND PROOF OF PRINCIPLE OF EXON-SKIPPING THERAPY

The principle of exon-skipping therapy for dystrophinopathies was initially demonstrated by Dunckley et al[8] in cultured mouse muscle cells in vitro. The rationale is as follows. Duchenne muscular dystrophy is caused by mutations of the 79-exon gene (commonly deletions of ≥1 exon). Within the myofiber, the remainder of the gene will be transcribed and spliced together. However, if the triplet codon reading frame of the mRNA is not preserved, the resulting frame shift will lead to the failure of dystrophin protein production. Becker muscular dystrophy (BMD) is a clinically milder and more variable disease in which mutations of the dystrophin gene are commonly such as to preserve the translational open reading frame; thus, after splicing together, the remainder of the gene retains some ability to synthesize the dystrophin protein. The goal of exon-skipping therapies is to force the dysfunctional mRNA with out-of-frame mutations in a patient with DMD to skip (exclude) some additional exons. The loss of additional material directed by AO drugs restores the reading frame, changing a Duchenne out-of-frame transcript to a Becker in-frame transcript. Fortunately, most mutations in the dystrophin gene occur in parts that do not code for functionally essential regions of the protein.

This AO-mediated exon-skipping method has been developed and extensively tested on the dystrophic *mdx* mouse model of DMD. The *mdx* mouse harbors a nonsense mutation in exon 23 that prevents translation beyond this point in the transcript. Both local intramuscular injection and systemic delivery of a single AO targeted against exon 23 in the primary transcript excludes this exon from the mRNA, leaving an in-frame transcript that generates dystrophin expression and produces a degree of functional recovery. Intramuscular and systemic injections of AOs for exon splicing of a dog model of DMD have also been demonstrated with a novel cocktail AO strategy (T.Y., S.T., Q.-L.L., T.A.P., A.N., E.P.H., and Masanori Kobayashi, DVM, unpublished data, 2006-2008). The principle is similarly illustrated in humans; van Deutekom et al[9] reported single-site intramuscular injections of 2′-O-methyl AO chemistry in 4 boys with DMD, showing evidence of de novo dystrophin production at the injection site.

These data demonstrate that the key hurdles of achieving intracellular delivery and avoiding toxic effects can be cleared. A similar strategy is being explored in other diseases such as myotonia, human immunodeficiency virus, and spinal muscular atrophy.[10-12]

HURDLES IN BRINGING EXON SKIPPING TO STANDARD OF CARE

Exon skipping using AO drugs has rapidly emerged as the frontline therapeutic approach for DMD. How soon can we expect exon skipping to reach the neuromuscular clinic and standard of care? This approach is breaking new ground and raising challenges not encountered previously in drug development. Different patients have different mutations, and many AO sequences will need to be designed, tested, and FDA approved. Also, current genotype and phenotype data suggest that there may be good in-frame deletions and not-so-good in-frame deletions; simply restoring the reading frame may not be synonymous with restoring dystrophin protein function. The optimization of dystrophin function will likely require deletions of multiple exons, and this will require mixtures of different AOs—new territory for drug development and the FDA. The approach will require regular injections of large amounts of AO drug; what are the long-term toxic effects? Moreover, are the standard toxicity tests appropriate for sequence-specific drugs? Each of these hurdles is discussed briefly in the remainder of this review.

CERTAIN EXON DELETIONS MAY RETAIN MORE DYSTROPHIN FUNCTION THAN OTHERS

The molecular diagnostics of DMD and BMD frequently refer to the reading frame rule, where out-of-frame deletions are given a DMD diagnosis and in-frame deletions are given a BMD diagnosis. However, as many as 30% of patients with BMD do not adhere to this rule.[13] A thorough understanding of reading frames is critical for appropriate design of exon-skipping therapies, both so that the best AO can be given to the patient and so that an optimally functional dystrophin protein is produced as a result of the expected exon skipping. Currently, the best information from which to predict the capabilities of partially deleted dystrophins to rescue the DMD phenotype comes from analysis of the thousands of geno-

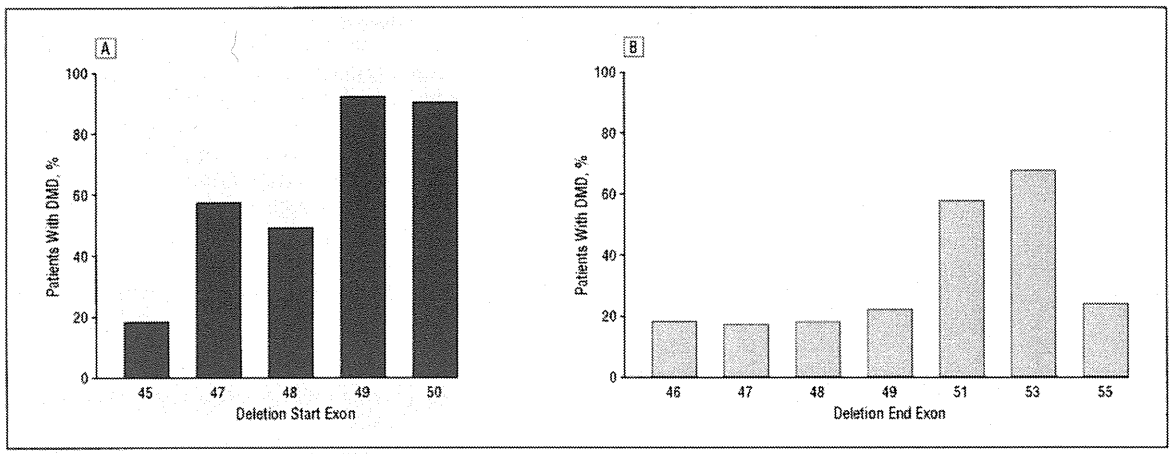

Figure 2. Clinical phenotypes associated with specific start (A) and end (B) sites for in-frame deletions. Percentages of patients with Duchenne muscular dystrophy (DMD) out of patients with DMD or Becker muscular dystrophy with specific start and end exons are shown. Combined muscular dystrophy databases of 14 countries (from Argentina, Belgium, Brazil, Bulgaria, Canada, China, Denmark, France, India, Italy, Japan, The Netherlands, the United Kingdom, and the United States) at Leiden University (http://www.dmd.nl), where diagnoses were performed using multiplex ligation-dependent probe amplification/multiplex amplification and probe hybridization, Southern blotting, or polymerase chain reaction primer sets that allow deletion boundaries to be assigned accurately to a specific exon, are used (deletion start sites: n=288 for exon 45, n=23 for exon 47, n=9 for exon 48, n=12 for exon 49, and n=10 for exon 50; deletion end sites: n=11 for exon 46, n=115 for exon 47, n=95 for exon 48, n=51 for exon 49, n=53 for exon 51, n=40 for exon 53, and n=21 for exon 55).

type and phenotype correlations in patients with DMD and BMD that have been published in the literature and on the Internet. We examined all in-frame deletions and determined the proportion of observed cases that showed mild or severe phenotypes. This was gleaned from combined muscular dystrophy databases of 14 countries (from Argentina, Belgium, Brazil, Bulgaria, Canada, China, Denmark, France, India, Italy, Japan, The Netherlands, the United Kingdom, and the United States) at Leiden University (http://www.dmd.nl), excluding diagnoses that did not allow deletion boundaries to be assigned accurately to a specific exon.[14] Of all observed in-frame deletion patterns on genomic DNA in the central rod domain hotspot region (exons 42-57; 28 distinct patterns), 57% (16 of 28 patterns) were associated with DMD rather than BMD. This analysis showed that there are considerable discrepancies between population-based ratios and pattern-based proportions of severe DMD vs mild BMD phenotypes, and interestingly, the ratio of DMD to BMD remarkably varies between specific deletion patterns. For example, in-frame deletions starting or ending around exon 50 or 51 that encode the hinge region were most commonly associated with severe phenotypes (**Figure 2**) (eg, deletions at exons 47-51, 48-51, and 49-53 are all reported to be associated with a severe DMD phenotype rather than BMD).[15,16]

Two questions arise. First, why do specific patterns of in-frame mutations tend to result in a severe DMD phenotype in contradiction to the reading frame rule? Second, why do different individuals with the same exonic deletion pattern exhibit such different clinical phenotypes? Likely contributory factors include the following: the effect of the specific deletion breakpoints on mRNA splicing efficiency and/or patterns; translation or transcription efficiency after genome rearrangement; and stability or function of the truncated protein structure. The mechanisms controlling accurate splicing of the 79-exon, 2.4 million–base pair dystrophin gene are clearly complex. Introns of the dystrophin gene are highly variable in size, and it is likely that exonic splicing does not take place in an ordered 5′ to 3′ sequence. A complication in interpreting genotype and phenotype correlations is that the deletion in genomic DNA does not always correspond to the material missing from the resulting mRNA. We and others have shown that even in the absence of AOs, a patient may produce 1 or more transcripts that skip additional exons present in the genomic DNA, in effect performing their own private exon skipping.[13] Disruption of splice site information (such as an intervening sequence) in some patients with in-frame gene deletions may cause skipping of additional exons at mRNA splicing, thus leading to out-of-frame transcripts from an in-frame genomic DNA deletion as Kesari et al[13] have recently described. As Menhart[17] has pointed out, it is also likely that quasi-dystrophin variants in the rod domain may show different stability or function because of different types of derangement of spectrinlike repeat domains. Not enough is known about dystrophin structure and function, and the relative importance of the protein sequence within the rod domain remains entirely a matter of speculation. Historically, lack of dystrophin expression has been used as the key criterion for DMD diagnosis. This together with the presence of the DMD clinical picture with such in-frame mutations argues that other confounding variables such as imprecisely defined mutation or aberrant splicing may explain these "exceptions to the reading frame rule." Thus, it is anticipated that most or all patients with mutations in the central rod domain would benefit from the production of truncated dystrophin.

PARALLELING AO TRIALS: TESTING NEW EXONS AND MIXTURES

Clinical proof-of-concept trials testing limited intramuscular injection with a 2′-O-methyl AO against exon 51

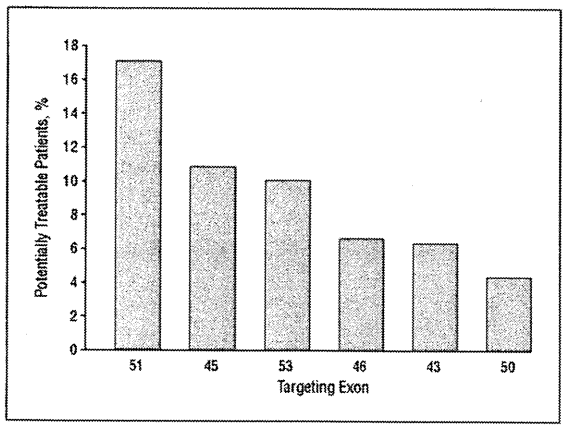

Figure 3. Targets of exon skipping and population of potentially treatable patients. Percentage of patients with the dystrophin deletion who are potentially treatable by targeting specific exons for Duchenne muscular dystrophy. For example, 17% of patients with Duchenne muscular dystrophy who have the dystrophin deletion can be potentially treated by targeting exon 51 using antisense oligonucleotides.

have been published,[9] and similar studies with PMO chemistry are under way in the United Kingdom. Given the many questions concerning the sequence specificity of toxic effects and the large number of AO sequences that will need to be developed as drugs to treat most patients with DMD, it is critical to parallel studies on many more AOs for DMD (**Figure 3**).

It should be noted that about 30% of patients with DMD have nondeletion mutations (duplication, nonsense mutations, small rearrangement, or splice site mutations). Most mutations are theoretically amenable to exon skipping; however, there are no hot spots for point mutations, so relatively few patients would be treatable with each targeted exon by comparison with deletion mutations. Moreover, if skipped to remove a nonsense mutation, the exons that are candidates to restore the reading frame in patients with deletions (eg, exons 43, 45, 46, 50, 51, and 53) will require additional deletion of at least 1 further exon to restore the reading frame because these are frame-shifting exons. Thus, only 35% of nonsense mutations are potentially treatable by single-exon targeting, but the combined data of the Leiden DMD mutation database imply that more than 90% could be responsive to multiskipping.[14]

Development of exonic cocktails (mixtures) could resolve a number of problems, including optimization of dystrophin function and covering relatively high proportions of patients with DMD with a single mixture. The mixture approach has clear advantages and disadvantages. As an example, an 11-exon AO cocktail skipping exons 45 through 55 is predicted to result in a particularly mild BMD phenotype (94% of reported patients).[14] Encouragingly, this large deletion is regularly associated with clinically milder phenotypes than any of the smaller in-frame deletions within the same range of exons 45 to 55.[18] A second advantage is that the cocktail could conceivably be approved as a single drug for most patients with DMD who have dystrophin deletions, independent of their precise deletion, eg, an 11-exon AO cocktail targeting exons 45 through 55 is potentially applicable to more than 60% of patients with a dystrophin deletion (**Figure 4**).[18,19] In total, more than 90% of patients with DMD could potentially be treated by multiskipping, whereas single-exon skipping could treat around half of the patients with dystrophin deletions and point mutations. Systemic studies in the large dog model of DMD have been done using a 3-exon PMO cocktail, and this has clearly been shown to be efficacious by multiple clinical, imaging, histological, and biochemical or molecular end points (T.Y., S.T., Q.-L.L., T.A.P., A.N., E.P.H., and Masanori Kobayashi, DVM, unpublished data, 2006-2008).

A disadvantage of the cocktail approach is the addition of novel hurdles for FDA or regulatory approval. Current FDA regulations require each component of a drug mixture to undergo toxicological and clinical testing and then require the mixture to similarly undergo toxicological and clinical testing. In the context of an ideal 11-exon AO cocktail, the regulatory barriers become truly intimidating. In addition, the 11-exon cocktail PMO approach would lead to delivery of some AOs that may not have a target in a specific patient (eg, the patient already has a deletion of ≥ 1 exon in the AO mix). Thus, some parts of the mixture will have no possible potential molecular or clinical benefit to individual patients. This would again be uncharted territory for the FDA. While clinical development of the 11-exon mixture is likely ambitious at present, it will be important to initiate toxicological and clinical trials of exon mixtures for subsets of patients who cannot be treated with a single AO. Also, for future trials on multiskipping such as with exons 45 through 55, we should have as many AOs in hand as possible because they can be used as part of multiskipping AOs.

PERSONALIZED MEDICINE AND THE FDA: ARE EXISTING GUIDELINES APPROPRIATE?

Personalized medicine has many definitions, but most share the concept of optimizing a treatment for a particular patient. Designing and using AO drugs targeted for a patient's specific gene mutation would seem to fit well within this rubric. As such, the promising AO exon-skipping approach may bring neuromuscular disease to the frontline in development of drugs for personalized medicine. It is important to examine the existing FDA guidelines for drug development and reinterpret these guidelines in the context of AO and DMD. For example, the drug development pipeline includes phase 1 studies of the drug in healthy volunteers. However, successful on-target exon skipping of the dystrophin gene in healthy volunteers would give them DMD, a clear adverse effect that is entirely irrelevant to toxic effects in the target patient population (boys with DMD). Toxicity tests are currently done in animal models (typically 2 species), but one of the major concerns regarding toxic effects of AO drugs is binding to off-target RNAs. For example, if an AO drug designed for exon skipping of the dystrophin mRNA also binds to the closely related utrophin mRNA, then exon skipping of utrophin might occur and could result in off-target adverse effects. The utrophin sequence of mice or rats is different from the utrophin sequence of humans, so the standard rodent toxicity tests